RE-EDUCATION OF TUMOR-ASSOCIATED MACROPHAGES VIA TLR7/8 AGONIST-ENCAPSULATED LIPOSOMES

A THESIS SUBMITTED TO

THE GRADUATE SCHOOL OF ENGINEERING AND SCIENCE

OF BILKENT UNIVERSITY

IN PARTIAL FULFILLMENT OF THE REQUIREMENTS FOR

THE DEGREE OF

MASTER OF SCIENCE

IN

MATERIALS SCIENCE AND NANOTECHNOLOGY

By

Eylül Tabel

September 2023

ABSTRACT

RE-EDUCATION OF TUMOR-ASSOCIATED MACROPHAGES VIA TLR7/8 AGONIST-ENCAPSULATED LIPOSOMES

Eylül Tabel
M.S. in Materials Science and Nanotechnology
Advisor: Bülend Ortaç
Co-Advisor: Gürkan Yeşilöz
September 2023

Cancer is an extremely complicated disease, and even though there have been years of effort in science to understand and find a cure, it still is one of the most terminal conditions. Lately, it is more clearly understood that the intricate wiring of the tumor microenvironment is more determinative than the intrinsic cancerous nature of tumor cells, for both disease prognosis and treatment efficiency. This environment bears many types of non-cancerous cells; such as endothelial cells, fibroblasts, and immune cells; all of which become heavily influenced by the cancer cells through their wiring of the cancer-helping niche. As proved by the success of a cancer staging approach, that utilizes a quantification of the infiltration of cytotoxic T cell populations, and which often offers a more effective staging system than traditional TNM staging for cancer, the low immunogenicity of the tumor microenvironment has been a new focus of target for kinds of therapies, including cytotoxic and immune-system stimulation approaches.

One such approach is targeting tumor-associated macrophages, which are highly specialized immune cells in the tumor microenvironment responsible for many biological functions such as proliferation of cancer cells, enhancement of cancer stemness, metastasis, and a low immunogenic profile around the environment. Amongst many strategies against these cells that have extraordinary polarization and switch-of-function capabilities, polarizing them back to a tumor-fighting polarization via stimulatory molecules have yielded promising results, with the biggest obstacle of induction of a systemic immune response.

Here, we have utilized liposomal encapsulation of a Toll-Like Receptor 7/8 agonist called resiquimod, in order to re-educate THP-1 macrophages that transformed into tumor-associated macrophages, back to an opposite state where they could no longer be allies of cancer cells. We have characterized the liposomes by size and morphology, and obtained a 200nm size. After we showed that this size ensured selective phagocytosis by macrophages; we loaded resiquimod molecules inside the liposomes through remote loading, with a loading efficiency of 96%. Tumor-associated macrophages that were obtained by HT-29-conditioned media incubation of THP-1 cells were characterized for their polarization state, and were re-educated with resiquimod-encapsulating liposomes. The efficiency of re-education was assessed by the reversal of tumor-associated polarization's impact on HT-29 cells in proliferation in standard cell culture by coverage assay and in spheroid culture, cell viability by flow cytometry, metastatic capabilities by wound-healing assay, and stemness by immunocytochemistry for CD133.

Overall, with a limitation of variety of tests to assess biological functions of the re-education, we have obtained promising results for an immunotherapeutic approach of re-educating tumor-associated macrophages in colorectal cancer.

Keywords: Tumor-associated macrophages, Resiquimod, Liposomes

ÖZET

TÜMOR-İLİNTİLİ MAKROFAJLARIN TLR7/8 AGONİSTİ YÜKLENMİŞ LİPOZOMLAR İLE YENİDEN EĞİTİMİ

Eylül Tabel
Materyal Bilimi ve Nanoteknoloji Bölümü, Yüksek Lisans
Tez Danışmanı: Bülend Ortaç
İkinci Tez Danışmanı: Gürkan Yeşilöz
Eylül 2023

Kanser, yıllardır üzerinde yapılan sayısız çalışmaya rağmen, karmaşık doğasıyla halen en ölümcül hastalıklardan biridir. Son zamanlarda kanserin prognozunda ve tedavisinin başarısında kanser hücrelerinin yapısal değişikliklerinden daha belirleyici bir öge olarak, tümör mikro-ortamının spesifik örüntüsü dikkat çekmiştir. Bu ortam kanser olmayan birçok hücre barındırır; endotel hücreler, fibroblastlar ve bağışıklık hücreleri bunlardan bazılarıdır ki tüm bu hücreler kanser hücrelerinin ağır etkisi altında, kansere yardımcı bir fenotipte bu mikro-ortamın karakteristiklerini oluştururlar. Klinikte en sık şekilde uygulanan TNM sisteminden bile daha efektif bir sınıflandırma sistemi olarak başarısını kanıtlamış bir sistemin yalnızca katı tümör ortamındaki sitotoksik T hücrelerinin dağılımını tespitten yola çıkması, tümörün immünojenitesinin yalnızca immünoterapötik yaklaşımlarda değil, geleneksel sitotoksik tedavilerde de ne kadar önemli olduğunu ortaya koymuştur.

Tümörün azaltılmış immünojenitesini değiştirmeye dayalı tedavi stratejilerinden biri, tümör-ilintili makrofaj hücrelerini hedef alır. Bu makrofajlar yüksek plastik kapasiteleriyle tümör ortamının etkisiyle farklılaşmış, kanserin ilerleyişine çeşitli

şekillerde destek olan hücrelerdir. Özellikle tümör hücrelerinin çoğalmasında, kök hücre karakterlerinin artmasında, metastazın desteklenmesinde ve ortamın immünojenitesinin azaltılmasında fazlasıyla etkili oldukları bilinmektedir. Bu hücreleri, tümöre yardımcı yerine tümöre karşı bir polarizasyona çevirmek yöntemiyle birçok umut verici sonuç elde edilmişse bile, sistemik enflamasyon riski nedeniyle birçoğu klinikte sınırlı şekilde kullanılmaktadır.

Bu çalışmada tümör-ilintili fenotipe çevrilmiş THP-1 makrofajların, lipozom partiküllerine yüklenmiş resiquimod (Toll benzeri reseptör 7/8 agonisti) molekülleri ile yeniden polarizasyonu hedeflenmiştir. Lipozomların üretim aşamasını takiben boyutları 200 nm olarak karakterize edilmiş, morfolojileri elektron mikroskobu ile gösterilmiş, makrofajlar tarafından seçici fagositozları analiz edilmiş ve ardından içlerine uzaktan yükleme metodu ile resiquimod molekülleri %96 oranında bir başarıyla yüklenmiştir. THP-1 makrofajlarının HT-29-şartlanmış-medya ile inkübasyonu ardından tümör-ilintili fenotipe evrimleri incelendikten sonra, üretilen lipozomlar ile yeniden polarizasyonu, HT-29 hücrelerinin üzerindeki biyolojik etkileriyle gözlemlenmiştir. Edindiğimiz bulgulara göre, yeniden polarizasyon, tümör-ilintili makrofajların HT-29 hücrelerindeki çoğalmayı ve canlı hücre sayısını arttırıcı, migrasyonu destekleyici ve kök hücre karakterini yükseltici etkilerini kısmi olarak tersine çevirmiştir.

Sonuç olarak, her bir biyolojik fonksiyona yaklaşımda kullanılan yöntemlerin çeşitlerindeki limitasyona rağmen, kolorektal kanser tümörlerdeki tümör-ilintili makrofajların polarizasyonunun tersine döndürülmesine dayalı bir immünoterapötik yaklaşım sunulmuş, ileride sistemik uygulama için üzerinde çalışılabilecek bir sistem olarak etkinliği ortaya konmuştur.

Anahtar Kelimeler: Tümör-ilintili makrofajlar, Resiquimod, Lipozomlar

Acknowledgement

Words cannot express my gratitude to my supervisor Dr. Gürkan Yeşilöz for his invaluable trust and patience with me throughout the process. It is thanks to him, that from being an undergraduate with little research experience, I have come so far in the way of becoming the scientist I want to be. I would also like to express that this endeavor would not have been possible without the generous support from Tübitak's International Fellowship for Outstanding Researchers Programme.

I would like to extend my sincere thanks to Servin Bagheralmoosavi, who not only teached me so much in the lab, but also encouraged me to move on when I needed. Without her, I would not be able to complete this work. Thanks should also go to Dr. Iqra Munir, for bearing with me each time I needed her help, and offering her generous insight and experience. I had the pleasure of working with a team that was extremely supportive with a positive attitude, and did not hold back their valuable contributions in discussions on the work, even when academic interests do not intersect. I appreciate them deeply.

I thank my beautiful mother, who never deprived me of her unconditional love, always got my back and made sure I feel her presence from miles away; and my father, who did his best to support me in every way possible. I cannot imagine how I would deal with all the happy and sad moments of this three-year journey, without Birsen. I am grateful to her for always being there for me. I am also thankful to Victor, my bunny, for his patience with the long hours I have spent away. I am extremely lucky to have such a great family.

Contents

1 Introduction 1

2 Methodology 9

2.1 Experimental Strategy 9

2.2 Equipment and Consumables 14

2.3 Cell Culture Experiments 17

2.3.1 Cell lines, Reagents, Solutions 17

2.3.2 Protocols of Cell Culture Experiments 20

2.3.2.1 THP-1 Monocyte Suspension Culture 20

2.3.2.2 Transformation of THP-1 Monocytes to THP-1 Macrophages 20

2.3.2.3 Transformation of THP-1 Macrophages into Tumor-Associated-Macrophages 20

2.3.2.4 Surface Culture of HT-29 Cells 21

2.3.2.5 Conditioned Media Incubations of HT-29 Cells 21

2.3.2.6 Spheroid Culture of HT-29 Cells 21

2.3.2.7 F-Actin and DAPI Staining 22

2.3.2.8 Immunocytochemistry 22

2.3.2.9 Flow Cytometry 23

2.3.2.10 Wound-Healing Assay 25

2.3.2.11 Coverage Assay 26

2.4 Liposome Studies 26

2.4.1 Chemicals, Reagents, Buffers 26

2.4.2 Protocols of Liposome Experiments 27
2.4.2.1 Liposome Production 27
2.4.2.2 Size Characterization of Liposomes by Dynamic Light Scattering 27
2.4.2.3 Morphological Characterization of Liposomes by Scanning Electron Microscope 28
2.4.2.4 Resiquimod Encapsulation by Liposomes 28
2.4.2.5 Quantification of Liposome-Encapsulated Resiquimod by Quadrupole Time-of-Flight Mass Spectroscopy (qTOF-MS) 28
2.4.2.6 Liposome Phagocytosis Assay 29
3 Results 30
3.1 Resiquimod-Loaded Liposome Characterization 30
3.2 Transformation of THP-1 Macrophages into Tumor-Associated Polarization 35
3.3 Re-Education of Tumor-Associated Macrophages by Resquimod-Encapsulating Liposomes 40
4 Discussion and Future Perspective 50
Bibliography 54

List of Figures

Figure 1. An overview of the study. 8
Figure 2. Workflow of production of liposomes, and sets of characterizations done at different steps. 10
Figure 3. Encapsulation of resiquimod by liposomes. 11
Figure 4. Transformation of THP-1 monocytes into THP-1 macrophages, followed by polarization to tumor-associated macrophage state by HT-29-conditioned media treatment. 12
Figure 5. Tumor-associated (TAM) and re-educated tumor-associated macrophage-conditioned media treatments on HT-29 cells, and consequent characterizations of malignant capabilities of cancer cells. 14
Figure 6. Size distribution of non-size-homogenized (i) and ultasonication-based size-homogenized liposomes (ii) by DLS analysis. 30
Figure 7. SEM images of the size-homogenized liposomes. 31
Figure 8. Fluorescence and bright observation of dye and liposomes alone, as well as dye-incubated and dialyzed liposomes, to show for labeling of liposomes. 32
Figure 9. Phagocytosis assay of liposomes by THP-1 macrophages (in tumor-associated polarization) and HT-29 cells. 32
Figure 10. Spectra found by qTOF-MS analysis of free resiquimod (i) and lysed resiquimod-encapsulated liposomes (ii). 34
Figure 11. Bright-field analysis of non-transformed (M0) and HT-29-conditioned media treated macrophages (TAM) on three consecutive days. 36
Figure 12. Analysis of cytoplasmic spread of non-transformed (M0) and HT-29-conditioned media treated macrophages (TAM). 37

Figure 13. Flow cytometry analysis to detect CD86+ and CD163+ macrophage populations of non-transformed (M0) and HT-29-conditioned media treated macrophages (TAM). 38
Figure 14. Immunocytochemistry for CD86 and CD163 receptors on non-transformed (M0) and HT-29-conditioned media treated macrophages (TAM). 39
Figure 15. Bright-field and F-actin with DAPI staining for morphological assessment of treatments done on tumor-associated macrophages (TAMs)..... 41
Figure 16. CD163 immunocytochemistry analysis for morphological assessment of treatments done on tumor-associated macrophages (TAMs)..... 42
Figure 17. Bright-field images of confluent HT-29 cells cultured in DMEM and confluent HT-29 cells cultured in RPMI 1640 for more than 5 passages. 43
Figure 18. Bright-field and respective F-Actin and DAPI staining analyses of HT-29 cells. 44
Figure 19. Coverage assay analysis of HT-29 cells..... 45
Figure 20. Flow cytometry analysis to detect dead and viable HT-29 cells..... 46
Figure 21. Growth analysis of HT-29 spheroids. 47
Figure 22. Wound-healing analysis of HT-29 cells. 48
Figure 23. Fluorescence images, of immunocytochemistry for CD133 complemented with F-actin and DAPI staining of HT-29 cells..... 49

List of Tables

Table 1. The list of equipment utilized in the study. 15
Table 2. The list of consumables utilized in the study. 16
Table 3. The list of filters with peak emission values utilized for fluorescence observations. 17
Table 4. Cell lines used in the study. 17
Table 5. The list of reagents used in maintenance of cell culture. 18
Table 6. The list of antibodies used in flow cytometry and immunocytochemistry experiments. 18
Table 7. The list of other reagents and chemicals used in cell culture experiments. 18
Table 8. Media and buffer specifications for cell culture. 19
Table 9. Antibody dilutions for immunocytochemistry experiments. 23
Table 10. Antibody dilutions for flow cytometry experiments. 25
Table 11. The list of chemicals, reagents and buffers in liposome studies. 26

List of Equations

Equation 1. Formula for drug encapsulation efficiency calculation by analysis of intensity values depicted in qTOF-MS. 33
Equation 2. Encapsulation efficiency calculation for resiquimod-encapsulated liposomes, using intensity values of the peaks in qTOF-MS analysis. 34

Chapter 1

Introduction

Many theories on cancer pathogenesis and concurrent therapeutic approaches have been emerging for many decades; making it one of the most heavily researched diseases of all times. Yet the current rates of therapy failure for most aggressive and later-stage cancer cases are around 90% (±5) (Maeda & Khatami, 2018). Alongside problems associated with drug development and low clinical translatability of scientific findings, one fundamental reason for such low success has been an incomplete understanding of the disease. For many years, certain genetic and epigenetic conditions were considered as the main root; yet even though they are necessary for cancer initiation and progression, it is now understood that they are inadequate (Bejarano et al., 2021; de Visser & Joyce, 2023). Microscopic examinations reveal a highly structured microenvironment collectively wired by both malignant and non-malignant cells embedded in an altered, aberrantly vascularized extracellular matrix (de Visser & Joyce, 2023). The non-malignant cells, including many types of immune cells, cancer-associated fibroblasts, endothelial cells, pericytes, and in some cases adipocytes and neurons, were initially thought as ineffective bystanders while aggressive cancer cells make their way through advanced stages (de Visser & Joyce, 2023). Only in the latest decades, the tumor-suppressive or tumor-supporting components in the tumor microenvironment have been getting some well-deserved attention; and they had been proved at least as crucial as the intrinsic features of cancer cells, for the processes of cancer initiation, progression, invasion, intravasation, extravasation, and even the formation of pre-

metastatic niche (Anderson & Simon, 2020; Baghban et al., 2020; Q. Wang et al., 2023). To tackle how such help occurs, it is crucial to comprehensively analyze the composition and functional state of the tumor microenvironment, yet these depend on many variables; including patient-specific factors (González-Silva et al., 2020; Pan & Jia, 2021; Q. Wang et al., 2023), the organ in which the tumor arises (Klemm et al., 2020; Schneider et al., 2017), the nature of cancer cells and their success in shaping the environment (Álvarez-Prado et al., 2023; Klemm et al., 2020), the distinct temporal and spatial distribution of types of cells in the environment, their secretome, cell surface receptor and ligands, and abundance of extracellular vesicles (Spranger & Gajewski, 2018; Wellenstein & de Visser, 2018). Despite such level of complexity, from the most initial steps of tumor formation to the latest stages of carcinogenesis; in the oncology clinic, one commonly determinative characteristic of the environment is the state of inflammation and the level of immunogenicity (Blankenstein et al., 2012; Multhoff et al., 2012; Singh et al., 2019; Zhao et al., 2021).

It was first demonstrated around twenty years ago, that T cell infiltrates and interferon-gamma (a pro-inflammatory cytokine) signatures may predict tumor progression and invasion better than TNM staging system which is the global standard for classifying cancer spread (T describing size of the primary tumor and its invasion, N describing regional lymph nodes involved, and M describing distant metastasis) (Galon et al., 2006). Numerous following clinical studies further validate that T cell infiltration and levels of pro-inflammatory cytokines are key determinants at the tumor microenvironment for the prognosis of the disease, which led to the crude definitions of cold and hot tumors to indicate the level of immunogenicity (hot being inflamed and high immunogenicity, and cold being the opposite) (Bindea et al., 2013; Fridman et al., 2012; Galon et al., 2006; Giraldo et al., 2014; Zhang & Zhang, 2020). These crudely defined states of the solid tumor then evolve into another classification system called Immunoscore that is based on quantification of two lymphocyte populations (CD3+ and CD8+) at two locations: the tumor center and the

invasive margin (Angell & Galon, 2013; Galluzzi et al., 2012; Galon et al., 2007; Pagès et al., 2018). A high Immunoscore indicates an immunologically hot tumor microenvironment, while a low Immunoscore defines a cold one -hence a lower immunogenicity and worse prognosis. Further investigations revealed an additional altered phenotype, which gives intermediate Immunoscore with T-cells found at the invasive margin, in some cases excluded from infiltration by physical hindrance, and in other cases excluded because of an "immunosuppressive" environment (Camus et al., 2009; Galon & Bruni, 2019). This immunogenicity-focused classification system has been validated globally in colon cancer first to have a greater prognostic value than lymphovascular invasion, tumor differentiation and micro-satellite instability status as well (Galon et al., 2013). Associated with the worst prognoses, the immunosuppressive nature of the cold tumors apparently leads the disease progression though not single-handedly, still too effectively to be overlooked.

This immunosuppression comes from the fact that T cells are not alone. Besides them, the tumor microenvironment bears many types of immune cells: primarily myeloid-derived suppressor cells, regulatory T cells and tumor-associated macrophages; all of which play substantial roles in wiring an unforgiving environment for cytotoxic T cells to enter and/or function properly (Bates et al., 2018; De Cicco et al., 2020). Tumor-associated macrophages undertake most of these roles. Those include downregulating TCR-associated ζ-chain, and over-expressing arginase-1 which catabolizes arginine (De Cicco et al., 2020) (an essential amino acid for CD4+ and CD8+ T cell activation), increasing reactive oxygen species and nitric oxide levels in the environment which influences many pathogenetic mechanisms like angiogenesis, tumorigenesis, apoptosis of regulatory T cells (Liou & Storz, 2010; Zhang et al., 2013) (apoptotic regulatory T cells impose a substantial immunosuppressive impact through oxidative stress-related mechanisms (Kraaij et al., 2010; Peng et al., 2021)), secreting cytokines like transforming growth factor-β and interleukin-10 (Jarnicki et al., 2006; Mirlekar, 2022) (they inhibit regulatory T

cells and critically impact immune homeostasis through metabolic signals (Cao et al., 2010; Levings et al., 2002)) as well as C-C motif chemokine ligands of CCL5, CCL20 and CCL22 which contribute to regulatory T cell recruitment to the microenvironment to exert even more of an immunosuppressive impact (Cui et al., 2020). Finding such environmental factors harsh, the T cells hardly make their way to the cancer cells (low Immunoscore) only to be silenced with mainly checkpoint inhibitors (intermediate Immunoscore). Besides the immunosuppressive roles, tumor-associated macrophages have lots of other functions throughout the whole pathogenesis (Yang et al., 2020), including nesting a cancer stem cell niche, meditating cross-talks between various types of cell types, extracellular matrix degradation during invasion, chaperoning circulating tumor cells, providing a convenient embedding and microenvironment wiring at the secondary tumor site.

As much as necessary it is to tackle these mechanisms for a more comprehensive picturing of the complex pathogenesis of cancer; the immunosuppressive and tumor-accommodating morphologies of tumor-associated macrophages make invaluable targets in treatment strategies. Such methodology is also ground-breaking to complement T-cell mediated immunotherapies; such as (Waldman et al., 2020): immune checkpoint therapy (particularly on inhibiting programmed cell death protein 1 and cytotoxic T lymphocyte associated molecule-4; PD-1 and CTL-4 respectively), adoptive T cell transfer therapy (through two types of genetically modified T cells: chimeric antigen receptor-T cells and T-cell receptor-engineered T cells; CAR-T and TCR-T therapies respectively), cytokine therapies, cancer vaccines, and combination therapies. There have been countless success stories with these strategies leading to remission and prevention of relapse (Brahmer et al., 2012; Brentjens et al., 2013; Clay et al., 1999a, 1999b; Hellmann et al., 2018; Hodi et al., 2010; Jaffee et al., 2001; Kirkwood et al., 1996; Leach et al., 1996; Lee et al., 2015; Morgan et al., 2016; Porter et al., 2011; Rapoport et al., 2015; Robbins et al., 2011; Rosenberg et al., 1985, 1986, 1988; Rosenberg & Restifo, 2015; Salgia et al., 2003;

Soiffer et al., 1998; Tura et al., 1994); yet their clinical effectiveness even when combined with traditional cytotoxic therapies have been lower than first anticipated (Zhang & Zhang, 2020). As eyes turn to accuse the immunogenicity of tumor microenvironment, which can be assessed clinically by Immunoscore: coldness and hotness are non-surprisingly found to be determining the immunotherapy success rate besides the prognosis. Hence for a next take in cancer treatment, of turning the cold tumor microenvironments hot, tumor-associated macrophages make promising target candidates, because of the unmatched levels of cellular interactions and molecular pathways these cells can mediate.

Still in its infancy, there have been attempts on targeting tumor-associated macrophages, with the aim of repolarizing these cells into a pro-inflammatory state. Because macrophage polarization spectrum is often considered to have two polars of pro-inflammatory M1 and anti-inflammatory M2; the repolarization can also be phrased as re-education of M2-like tumor-associated macrophages into M1-like macrophages that no longer serves for the immunosuppression, recruit and dope cytotoxic T cells, and unwire the neatly wired tumor microenvironment. There have been good outcomes with this strategy, especially in activating CD4+ and CD8+ T cell-mediated immunity, and various methodologies have been developed. Amongst many, one pharmaceutical take is to utilize agonists for toll-like receptors, which are the key receptors in mediating the polarization state of macrophages.

Toll-like receptors belong to pattern recognition receptors family, and can recognize sets of pathogen-associated and damage-associated molecular patterns (Yu & Feng, 2018; Zhang & Liang, 2016). Expressed by innate immune cells, they stimulate various signaling cascades for both defense and repair (Y. Wang et al., 2016; Wong et al., 2009). Macrophages express these receptors heavily, and do rely on them often for switching between M1 and M2 polarizations. With well-known impact of such switch on development and progression of many diseases (Q.-Q. Huang & Pope,

2009; Jialal et al., 2014; So & Ouchi, 2010; Subramanian et al., 2006; Tsujimoto et al., 2008), using antagonists and agonists for these receptors is not a new concept (Gao et al., 2017; Jezierska et al., 2011; Montero Vega & de Andrés Martín, 2009), yet their use in oncological treatment is controversial (Adams, 2009; Farooq et al., 2021; Pahlavanneshan et al., 2021). The methodology and strategy for targeting depends on the receptor localization and the signaling pathway it induces on macrophages (X. Chen et al., 2022), as well as the other cells that might be expressing the receptor around the tumor microenvironment and hence the possibility of dual impacts in the heterogeneous and complex nature of that environment (Beury et al., 2014; Kaczanowska et al., 2013; T. T. Li et al., 2014). That said, the power of what these receptors can impose to transform tumor-associated macrophages make them attractive targets, and worthy of more research, for better immunotherapeutic strategies.

In this work, a TLR7/8 agonist, resiquimod, is tested as a therapeutic agent to transform tumor-associated macrophages into M1-like polarization state by the activation of MyD88-dependent signaling pathway. This agonist is an FDA-approved therapeutic molecule, with its efficiency shown for genital herpes, hepatitis C and actinic keratosis, skin cancer and cutaneous T cell lymphoma (Farr et al., 2021; Killock, 2015; Meyer et al., 2013; Rook et al., 2015), when applied topically on the lesions. It induces powerful activation on various disease-related immune components. Some patients even experience a systemic immune response through resiquimod-mediated activation of circulating dendritic cells through topical administration, which makes resiquimod the first topical medication that also regresses untreated skin lesions (Killock, 2015). Such strong impact this molecule can have poses problems for its further use, such as in non-topical administration, where systemic inflammation is unescapable.

In order to address this issue, we have utilized liposomal constructs to encapsulate resiquimod molecules. Liposomes are bilayer lipid membranes encapsulating an aqueous core in a spherical shape. Their high biocompatibility and biodegradability, low toxicity and immunogenicity, along with the plasticity in formulations (such as lipid compositions and surface modifications) make these vehicles great pharmaceutical agents (Abbasi et al., 2022; Deshpande et al., 2013; Liu et al., 2022). Especially for targeting solid tumors, owing to the pathophysiology of abnormal angiogenesis and consequent enhanced permeability and retention effect (Wu, 2021), liposomes make great choices for therapeutic carriers with a good retention rate on tumor site. This entails an impactful re-education of tumor-associated macrophages by resiquimod without invoking a serious systemic immune response, as resiquimod-encapsulated liposomes potentially aggregate in the tumor site, being prone to get phagocytosed by the tumor-associated macrophages. Besides those advantages; having the target receptors localized in the endosomal membrane of the macrophages, when the agonist is provided to the cells in liposomes with 200-1000nm diameter (which is an appropriate size range for selective phagocytosis by highly phagocytic cells), they would theoretically bind to their receptors in the phagolysosomes more effectively than in their free form.

An abstract scheme for the whole study is presented in Figure 1. Overall, we show that re-education of tumor-associated macrophages through resiquimod-encapsulating liposomes can reverse their tumor-accommodating impact to some level. Limitations include the variation of assays done to assess each malignant function, i.e. metastatic capabilities, proliferation rate, viability characteristics (identification of apoptosis, necrosis, metabolic stress, other ways of losing viability), stemness; as well as a starved characterization of tumor-associated macrophages in terms of surface receptor expressions and activated signaling pathways. In need of a great mass of further research, this work still points to a non-negligible potential in

targeting tumor-associated polarization states of macrophages around the tumor microenvironment of colorectal adenocarcinoma.

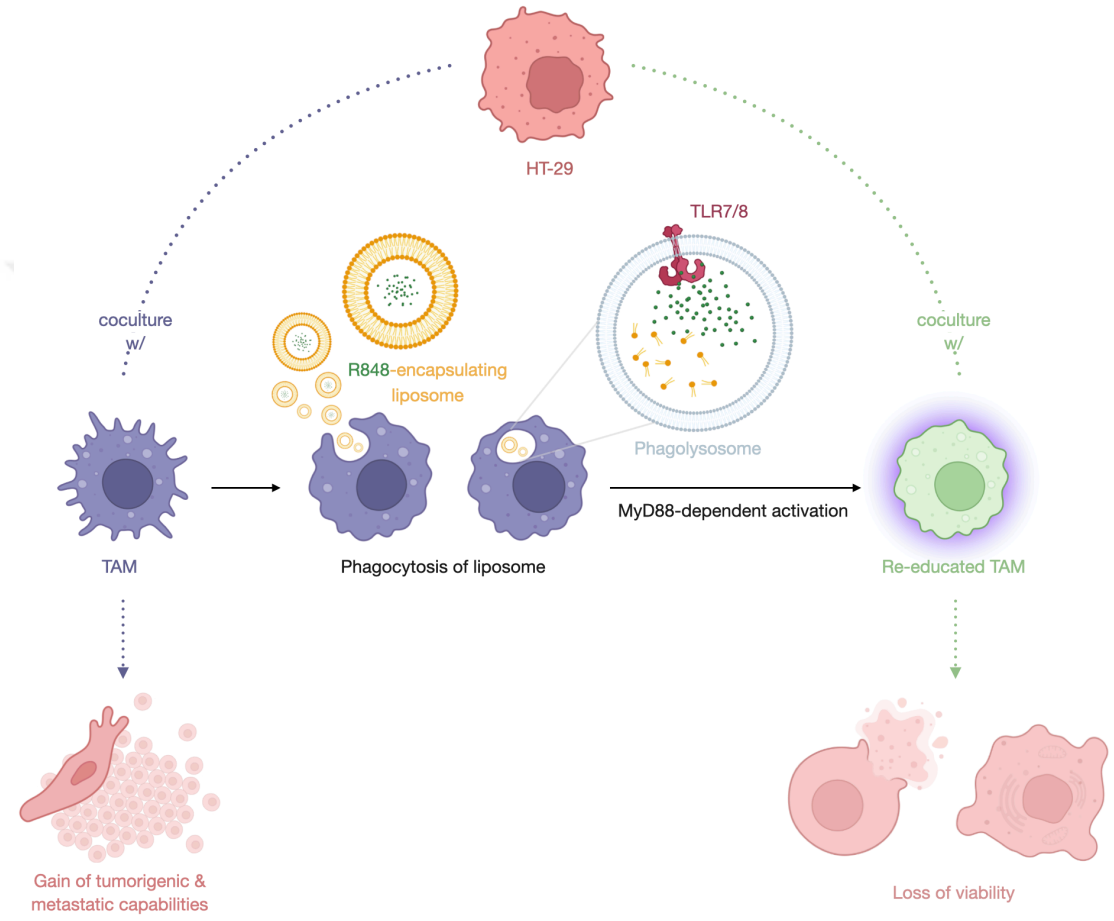

Figure 1. An overview of the study. THP-1 human monocytes from peripheral blood (acute monocytic leukemia) are turned into tumor-associated macrophages (TAM), and are re-educated with resiquimod (R848)-encapsulating liposomes to activate MyD88-dependent signaling pathway. The impact of re-education is shown by treating HT-29 human epithelial colon cells (colorectal adenocarcinoma) with TAM and re-educated TAM-conditioned media, and analyzing tumorigenic, metastatic and viability profiles of cancer cells. Scheme is designed in © BioRender.

Chapter 2

Methodology

2.1 Experimental Strategy

The study was divided into three main steps: production and characterization of resiquimod-encapsulating liposomes, transformation and characterization of tumor-associated macrophages, re-education of tumor-associated macrophages by resiquimod-encapsulating liposomes with characterization of the impact of the re-education on malignant capabilities of colorectal cancer cells, i.e., proliferation, viability, migration, and stemness.

Figure 2 summarizes the workflow for producing such resiquimod-encapsulating size-homogenous liposomes. Briefly, a lipid thin film made of two types of phospholipids was hydrated with ammonium sulfate, for subsequent transportation of the hydrophobic drug through remote loading (a chemical description of remote loading is drawn in Figure 3). Followed by sets of characterizations, which involves selective phagocytosis assay and physicochemical characterization of the liposomes; the liposomes were ready for treatment on cells.

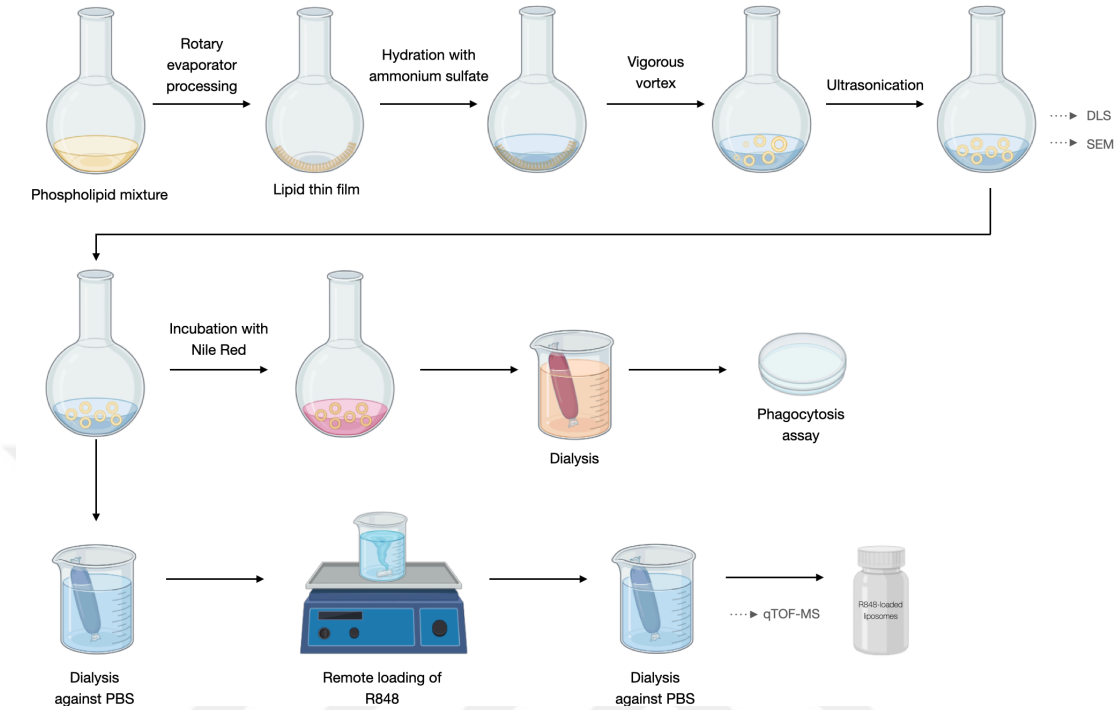

Figure 2. Figure 2. Workflow of production of liposomes, and sets of characterizations done at different steps. Briefly, lipid thin film hydration methodology was utilized, where hydration is done by ammonium sulfate solution to induce remote loading. To show for selective phagocytosis by macrophages, liposomes are labeled by lyophilic dye Nile Red. Scheme is designed in © BioRender.

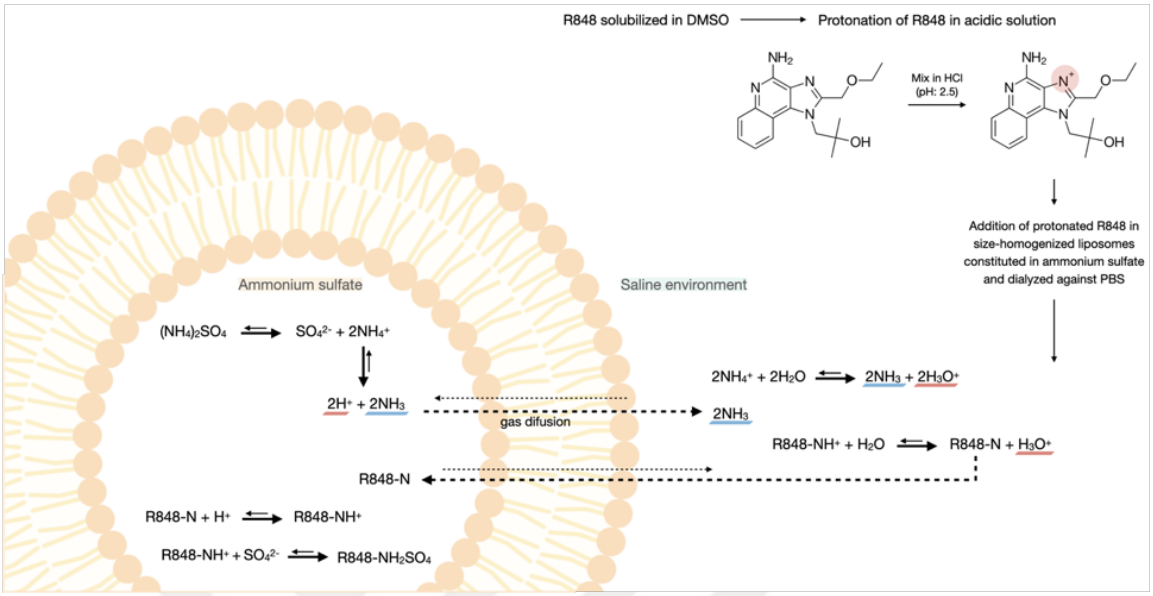

Figure 3. Encapsulation of resiquimod by liposomes. Liposomes with ammonium sulfate on the internal and saline on the external are incubated with protonated resiquimod (R848) molecules. Through an exchange of molecules across lipid bilayer membrane, a process called remote loading, resiquimod translocates to internal of the liposomes. Scheme is designed in © BioRender.

In the study, we included two cell lines: THP-1 human monocytes from peripheral blood (acute monocytic leukemia) and HT-29 human epithelial colon cells (colorectal adenocarcinoma). The rationale behind choosing these cell lines comes from a study [101] in which serial sections from 81 colorectal carcinoma patients have been examined to show clinical significance of tumor-associated macrophages in the disease, where it was found that the tumor invasive front contained most of the tumor-associated macrophages population and drove metastasis of the tumor. They were able to replicate similar marker expression levels by transforming THP-1 macrophages into tumor-associated macrophages by HT-29-conditioned media. Hence, we have first turned THP-1 monocytes into macrophages via incubation with Phorbol 12-myristate 13-acetate (PMA); and then were transformed into tumor-associated macrophages via incubation with HT-29-conditioned media (Figure 4).

We have characterized this transformation by assessing the expressions of surface receptors CD86 (indicative of an M1-like, pro-inflammatory polarization) and CD163 (indicative of an M2-like, anti-inflammatory polarization) through flow cytometry and immunocytochemistry techniques, as well as fundamental bright-field and F-actin-DAPI staining observations to analyze the transformed morphology. Both these markers were shown in the same study as the biomarkers of which the expressions have changed the most significantly (Wei et al., 2019).

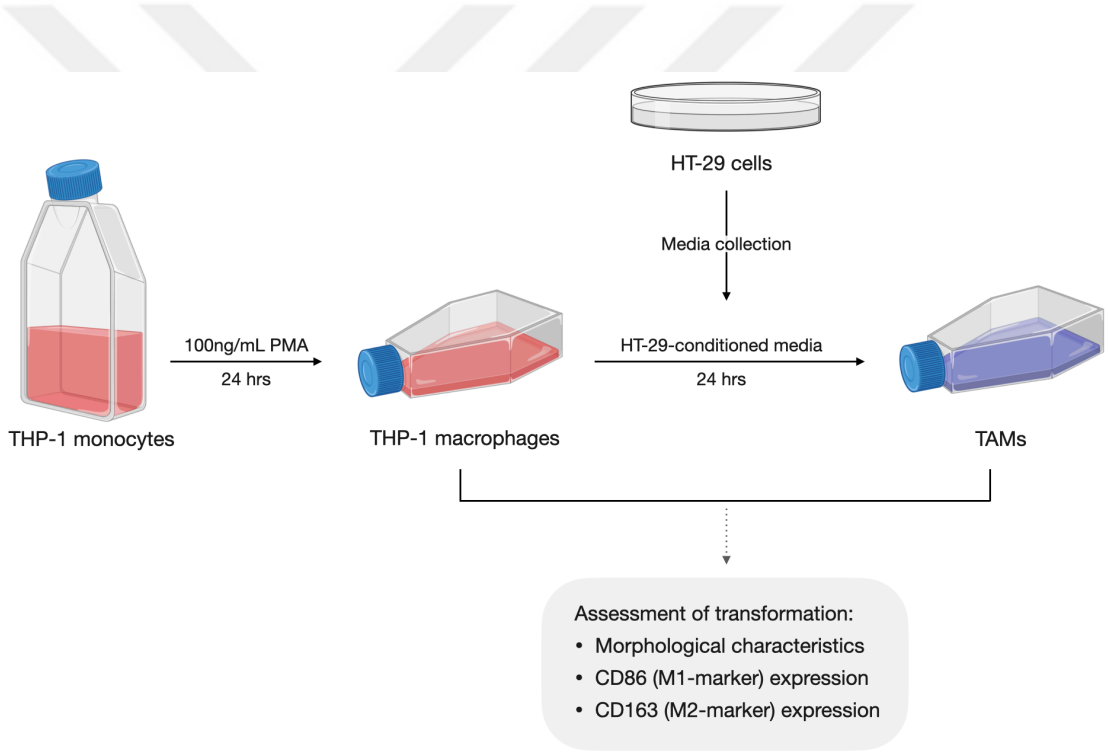

Figure 4. Transformation of THP-1 monocytes into THP-1 macrophages, followed by polarization to tumor-associated macrophage state by HT-29-conditioned media treatment. Methods for characterization of polarization state are also listed. Scheme is designed in © BioRender.

We have then treated tumor-associated THP-1 macrophages with R848-encapsulating liposomes, and discovered what impact they imposed on HT-29 cells differently than tumor-associated polarization could impose, to assess the re-

education efficiency (Figure 5). Even though such strategy doesn't necessarily reveal the change in immunogenic profile, because the pro-tumorigenic and metastatic roles of tumor-associated macrophages are well-known, we assume that showing how different of an impact these macrophages can exert on cancer cells through re-education would be indicative of the re-education success. For such qualification, we have analyzed the changes in stemness of HT-29 cells by CD133 immunocytostaining (a well-described cancer stem cell marker). Because tumor-associated macrophages can communicate with cancer stem cells and enhance stemness and proliferation, and drug resistance and cancer stem cell ratio are positively associated in the clinic, we have hypothesized that re-education of tumor macrophages would decrease the stemness and drug resistance. We have furthermore tested the impact on proliferation abilities of cells, in a coverage assay in two-dimensional, and a spheroid growth assay in three-dimensional culture of HT-29; and on viability of cells by flow cytometry analysis. Finally, a wound-healing assay is performed in order to assess the metastatic capabilities of the cancer cells. Thus, we aimed to draw a comprehensive picture of the general impact of such re-education, which have a good potential to make it to clinical trials, on one epithelial cell line of human colorectal adenocarcinoma.

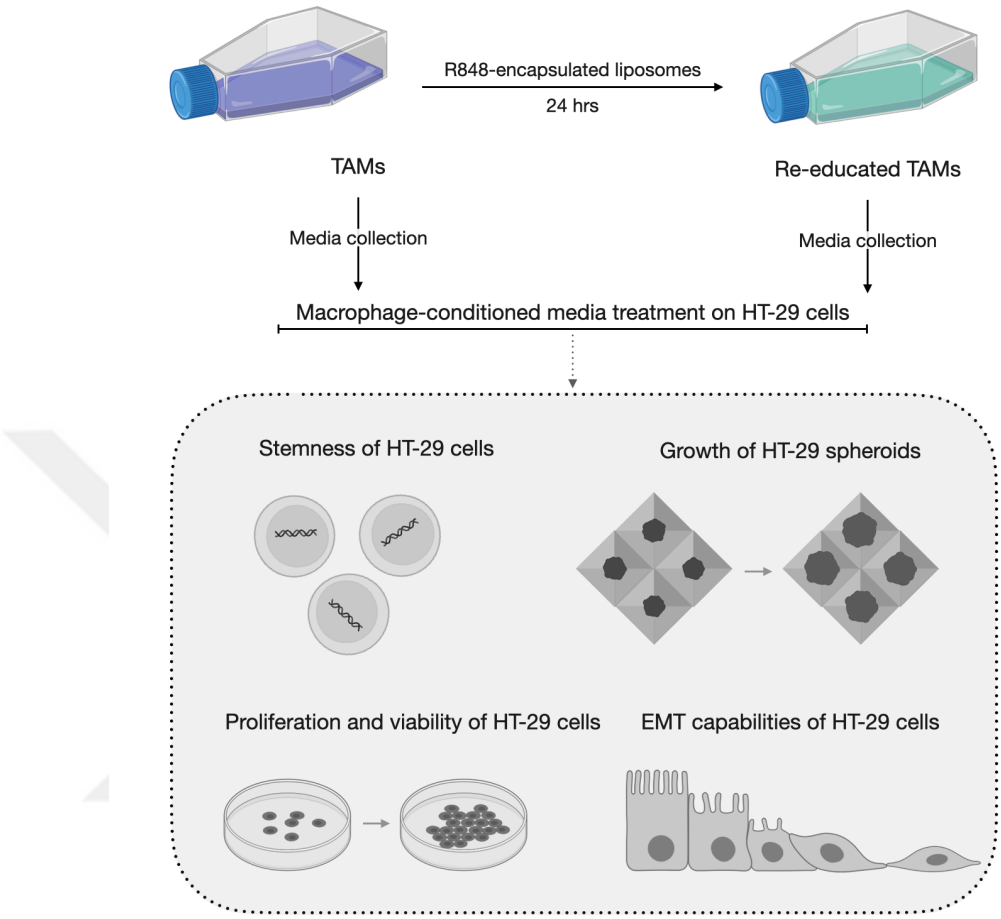

Figure 5. Tumor-associated (TAM) and re-educated tumor-associated macrophage-conditioned media treatments on HT-29 cells, and consequent characterizations of malignant capabilities of cancer cells. Scheme is designed in © BioRender.

2.2 Equipment and Consumables

In tables below, equipment (Table 1) and consumables (Table 2) utilized in the study are listed. The fluorescence microscope filters utilized are as depicted In Table 3.

Table 1. The list of equipment utilized in the study.

Equipment	Brand
Fluorescence Microscope	Carl Zeiss Axio Observer 7
Dynamic Light Scattering - Zeta Potential analyzer	Malvern Nanoseries-ZS
Environmental Scanning Electron Microscopy (E-SEM)	FEI Quanta 200F
Vacuum Coater for E-SEM	
Quadrupole Time-of-Flight Mass Spectroscopy	Agilent 1290 LC
Flow cytometer	BD Accuri
Cell scraper	Corning Incorporated
Biosafety cabinet	NUVE MN120
Cell culture incubator in 37°C with 5% CO_2	NUVE EC160
Water bath	NUVE NB9
Centrifuge	NUVE NF800
Vortex	IKA VORTEX 2
Cell counter	Thoma 610731
Ultrasonicator	Bandelin Electronic Typ: UW2070
Hot plate with magnetic stirrer	IKA C-MAG HS7
Weighing Balance	OHAUS
Micropipettes	BOECO
Rotary evaporator	Buchi Rotavapor R-100
Fume hood	Köttermann Systemlabor

Table 2. The list of consumables utilized in the study.

Product	Brand	Cat. No.
15 mL falcon tube	ABDOS	P10442
50 mL falcon tube	ABDOS	P10404
0.5 mL reaction tubes	Ultra Cruz	sc-200269
1.5 mL reaction tube	Ultra Cruz	sc-200271
Cryo-vial	ABDOS	P60108
5 mL serological pipette	ABDOS	P10603
10 mL serological pipette	ABDOS	P10604
50 mL serological pipette	CAPP	SP-50
Pipette tips	JET BIOFIL	PPT-000-000
6-well plate	SPL	30006
24-well plate	ISOLAB	12211006
96-well plate	ISOLAB	12211006
3cm culture petri dish	CORNING	3294
6cm culture petri dish	NEST	705001
10cm culture petri dish	NEST	704001
PVDF membrane filter (0.45um)	Labfil	C0000284
PTFE membrane filter (0.22um)	Labfil	C0000488
Microcuvettes	Biosigma	BSA002
Syringe (5mL)	Luer	B1903105

Table 3. The list of filters with peak emission values utilized for fluorescence observations.

Analysis	Filter (Peak Emission)
DAPI	465nm
F-actin	517nm
Nile Red	618nm
ABflo 647-conjugated Goat Anti-Rabbit IgG (H+L)	618nm
ABflo 555-conjugated Goat Anti-Mouse IgG (H+L)	568nm

2.3 Cell Culture Experiments

2.3.1 Cell lines, Reagents, Solutions

In tables below, cell lines (Table 4), reagents used in maintenance of cell culture (Table 5), antibodies (Table 6) and other reagents and chemicals (Table 7) utilized in cell culture experiments, as well as media and buffer specifications (Table 8) are listed.

Table 4. Cell lines used in the study.

Cell line	Organism	Morphology	Tissue	Disease
THP-1	Human	Monocyte	Peripheral blood	Acute monocytic leukemia
HT-29	Human	Epithelial	Colon	Colorectal adenocarcinoma

Table 5. The list of reagents used in maintenance of cell culture.

Product	Brand	Cat. No.
RPMI 1640 Culture Medium	SEROX	SLR-563-500
Fetal Bovine Serum	SERANA	46010323FBSP
Penicillin/Streptomycin	SERANA	01070121RAL
PBS	SERANA	01050621BDL
Trypsin-EDTA	SERANA	01112020RTL
Molecular biology-grade DMSO	SERVA	221147

Table 6. The list of antibodies used in flow cytometry and immunocytochemistry experiments.

Antibody	Brand	Cat. No.
Anti-Rabbit CD163/M130 antibody	Abclonal	A8383
Anti-Mouse CD86/1146 antibody	Biorbyt	orb12124
Anti-Rabbit CD133 antibody	Abclonal	A0219
ABflo 647-conjugated Goat Anti-Rabbit IgG (H+L)	Abclonal	AS060
ABflo 555-conjugated Goat Anti-Mouse IgG (H+L)	Abclonal	AS057

Table 7. The list of other reagents and chemicals used in cell culture experiments.

Product	Brand	Cat. No.
Phorbol 12-myristate 13-acetate (PMA)	MedChem	HY-18739
Bovine Serum Albumin (BSA)	PAN BIOTECH	P06-139310
Triton X-100	ABCR	1191772
Phosphate Buffered Saline (PBS)	SERANA	01050621BDL
Molecular biology-grade water	BioFroxx	1058LT001
Tryphan blue	SIGMA	RNBJ7454
Calcein-AM	Invitrogen	2256755

Propidium Iodide (PI)	Merck	P4170
DAPI	Sigma	MBD0015
F-actin	Thermo Fisher Scientific	2277811
Ethanol	Sigma-Aldrich	32221

Table 8. Media and buffer specifications for cell culture.

Solution	Content	Storage temperature
Media for HT-29 and THP-1 macrophage culture	89% RPMI 1640 10% FBS 1% Penicillin-Streptomycin	+4°C
Media for THP-1 monocyte culture	80% RPMI 1640 20% FBS	+4°C
Freezing media	90% FBS 10% DMSO	-20°C
Fixing buffer	96% PBS 4% Paraformaldehyde	+4°C
Permeabilization buffer	98.8% PBS 0.2% TritonX-100	Freshly prepared
Blocking buffer	97% PBS 3% BSA	+4°C
Flow cytometry buffer	99% PBS 1% BSA	+4°C

2.3.2 Protocols of Cell Culture Experiments

All cell culture experiments were conducted in the biosafety cabinet, and the cells were kept in incubation in the cell culture incubator at 37°C with 5% CO_2.

2.3.2.1 THP-1 Monocyte Suspension Culture

THP-1 monocytes were kept in nitrogen tank with 5 million cells/mL concentration in freezing media, and were thawed by four-fold dilution in cold RPMI, followed by pellet dissolution in warm culture media to start suspension culture. They were maintained in suspension culture, with a confluency range between 1,000,000 - 2,000,000 cells/mL. During freezing procedures, cell pellet was obtained by centrifugation for 5 minutes at 175 RCF, and cells were suspended with the given concentration in freezing media, and were placed in nitrogen tank.

2.3.2.2 Transformation of THP-1 Monocytes to THP-1 Macrophages

THP-1 monocytes were seeded on culture plates with a density of 100,000 cells per cm^2 surface, with 100 ng/mL PMA in their culture medium. After 24 hours, PMA-containing media incubation was terminated, and cells were either incubated in culture media, or were transformed into tumor-associated macrophages.

2.3.2.3 Transformation of THP-1 Macrophages into Tumor-Associated-Macrophages

After transformation into macrophages, PMA-containing media was replaced by HT-29-conditioned media, which was the media that HT-29 cells were incubated with during days between 50-80% confluence. Before use, HT-29-conditioned media was filtered through 0.44 μm PVDF membrane.

2.3.2.4 Surface Culture of HT-29 Cells

HT-29 cells were kept in nitrogen tank with 5 million cells/mL concentration in freezing media, and were thawed by four-fold dilution in cold RPMI, followed by pellet dissolution in warm culture media to start culture. They were maintained in culture starting from around 35000 cells/cm^2, and was passaged before reaching around 85% confluency, which took around 5-6 days. Passaging was performed by washing of cells with warm PBS for two times, followed by a coverage with trypsin-EDTA solution and incubation at 37°C for 4 minutes. Then trypsin was inactivated by addition of same volume of culture media (with 10% FBS), and was centrifuged for 5 minutes at 175 RCF. The resultant pellet was then counted and either passaged or suspended in freezing media and kept in nitrogen tank.

2.3.2.5 Conditioned Media Incubations of HT-29 Cells

For surface culture of HT-29 cells, upon reaching a confluency of 40%, culture media was replaced by either tumor-associated or re-educated-tumor-associated macrophage-conditioned media. This media was obtained by 24 hours incubation of media on macrophages, which was then filtered through 0.44 μm PVDF membrane. HT-29 cells were incubated in the conditioned media for 48 hours, before analysis.

2.3.2.6 Spheroid Culture of HT-29 Cells

In order to form spheroids, a customized mold was utilized to yield 24 micron-sized agarose wells in a 96-well plate well, as described in a protocol in literature (Krishnan et al., 2021). The wells had a shape of truncated square pyramid, where one corner of the square well was 500μm, the height of the microwell was 200-300μm, and one corner of the truncated base square was 300μm. 8,000 HT-29 cells in 200μL culture media were seeded on each well, and the plate was centrifuged for

5 minutes at 200 RCF. Media was changed every two days by slowly pipetting out 100µL from consumed media, and slowly pipetting in 100µL fresh culture media. Four days later, cells were observed to form tight cellular interactions having transformed from aggregates into intact spheroids. From then on, media was changed the same way every day with either macrophage-conditioned media or fresh culture media, for five consecutive days. Ten selected spheroids from four same-treatment wells were analyzed by the area they cover on microscope software, making forty spheroids per treatment, to reveal growth profiles.

2.3.2.7 F-Actin and DAPI Staining

All steps were followed at room temperature. For F-actin-DAPI staining, 2.5% F-actin was prepared in PBS, and 10µg/mL DAPI was prepared in PBS as working solutions. Culture media was aspirated, and the cells were washed twice with PBS, before being fixed in fixing buffer for 20 minutes in fume hood. Then the fixing buffer was aspirated, and cells were washed for 5 minutes with PBS, and incubated in permeabilization buffer for 5 minutes. After incubation time, permeabilization buffer was removed and the cells were washed again for 5 minutes with PBS. Then, cells were incubated in F-actin working solution for 30 minutes. F-actin solution was aspirated, and cells were washed for 5 minutes with PBS, before incubation in DAPI working solution for 10 minutes. Cells were then aspirated, washed for 5 minutes with PBS, and analyzed on fluorescence microscope with appropriate filters.

2.3.2.8 Immunocytochemistry

Culture medium was aspirated, cells were washed with PBS twice, and were fixed with 20 minutes incubation in fixing buffer in room temperature in the fume hood. They were aspirated, and washed with PBS for 5 minutes three times. Permeabilization buffer was added on cells, and they were left in incubation for 45

minutes at room temperature. During incubation, primary antibody dilution was freshly prepared in blocking buffer. Following permeabilization buffer aspiration and washes with PBS for 5 minutes three times, primary antibodies in blocking buffer were treated on cells. Cells were then incubated at 4°C overnight. The antibody solution was then aspirated and cells were washed with PBS for 5 minutes three times. During wash steps, at dark, secondary antibody dilution was freshly prepared in blocking buffer, and were treated on cells following the washing. The cells were incubated for 1 hour at room temperature, at dark. Cells were then aspirated, and washed with PBS for 5 minutes three times. For nuclear staining, the cells were incubated in 10µg/mL DAPI for 10 minutes at room temperature, at dark. They were aspirated and washed with PBS for 5 minutes, and were analyzed on fluorescence microscope with appropriate filters. The resulting images were analyzed for the fluorescence intensity on ImageJ, by measuring the ratio of the intensity of selected cell to cell area, for random cells.

Table 9 includes antibody dilutions used for immunocytochemistry experiments.

Table 9. Antibody dilutions for immunocytochemistry experiments.

Antibody	Dilution
Anti-Rabbit CD163/M130 antibody	1:100
Anti-Mouse CD86/1146 antibody	1:50
Anti-Rabbit CD133 antibody	1:200
ABflo 647-conjugated Goat Anti-Rabbit IgG (H+L)	1:200
ABflo 555-conjugated Goat Anti-Mouse IgG (H+L)	1:50

2.3.2.9 Flow Cytometry

Cells were detached from the surface using a cell scraper, and were then centrifuged once for 2 minutes at 300 RCF, and were suspended in 1mL flow cytometry buffer. After cell counting, they were aliquoted with 1 million cell/mL concentration, each aliquot having 1mL solution, in flow cytometry buffer, and were centrifuged again for 2 minutes at 300 RCF. The pellet was resuspended in 1mL flow cytometry buffer for washing, to be centrifuged for 2 minutes at 300 RCF. Then, pellet was resuspended in 1mL flow cytometry buffer.

For viability analysis, 100ng of Calcein-AM was added to the 1mL cell suspension. The cells were then incubated at 4°C for 15 minutes. After the incubation time, 2μg propidium iodide was added to the suspension, and was incubated at room temperature for 15 minutes. The cells were then analyzed on flow cytometry device.

For analysis with antibody labeling, primary antibody was added to the 1mL cell suspension. The cells were then incubated at 4°C for 30 minutes. After the incubation time, they were centrifuged for 2 minutes at 300 RCF, and were resuspended in 1mL flow cytometry buffer, and this washing step was done three times in total. After final wash, the suspended pellet was incubated with the secondary antibody at 4°C for 30 minutes. Then the cells were centrifuged for 2 minutes at 300 RCF, and were resuspended in 1mL flow cytometry buffer. They were then analyzed on flow cytometry device.

In Table 10, antibody dilutions utilized for flow cytometry experiments are listed.

Table 10. Antibody dilutions for flow cytometry experiments.

Antibody	Dilution
Anti-Rabbit CD163/M130 antibody	1:200 (5uL per 1,000,000 cells)
Anti-Mouse CD86/1146 antibody	1:100 (10uL per 1,000,000 cells)
ABflo 647-conjugated Goat Anti-Rabbit IgG (H+L)	1:500
ABflo 555-conjugated Goat Anti-Mouse IgG (H+L)	1:200

2.3.2.10 Wound-Healing Assay

HT-29 cells were cultured until around 90% confluency on a 24-well plate, and then were either treated with tumor-associated or re-educated tumor-associated macrophage-conditioned media, or were changed their regular culture media, for two more days to reach 100%. At the point of confluency, the cells monolayers were carefully scratched with the edge of micropipette tip in a shape of cross, and were vigorously washed with PBS to remove dead cells for three times. After washing, cells were added with RPMI 1640 with 1% FBS and 1% penicillin-streptomycin solution. The wells of the plate were pictured with respect to the position of the cross, and the straight scratches with similar sizes were selected. Wells were changed with the same media followed by and bright-field analysis of scratches from the same location using the cross as a reference, for consecutive four days. The culture was terminated, and the bright-field images were cleaned from the cellular debris at the scratched areas, and the non-covered area was measured in ImageJ to be divided by the total area of the taken image and multiplied by 100. Such that, non-covered area percentage was calculated for each condition.

2.3.2.11 Coverage Assay

HT-29 cells were cultured until around 40% confluency, and then were either treated with tumor-associated or re-educated tumor-associated macrophage-conditioned media, or were changed their regular culture media, for three more days. Each day of a total of four days, the cells were imaged on bright-field with 2.5X magnification. The images were analyzed on ImageJ, and area covered by cells was divided by the total image area, and multiplied by 100, to find area coverage percentage.

2.4 Liposome Studies

2.4.1 Chemicals, Reagents, Buffers

Chemicals, reagents and buffers used in liposome studies are listed in Table 11.

Table 11. The list of chemicals, reagents and buffers in liposome studies.

Product	Brand	Cat. No.
Resiquimod	MedChem	HY-13740
Phosphate Buffered Saline (PBS)	SERANA	01050621BDL
Molecular biology-grade water	BioFroxx	1058LT001
Nile red	Sigma	7385-67-3
Sunflower Phosphatidylcholine with 90% Phosphotidylcholine	Lipoid	533600-1160002-07/902
Sn-Glycero-3-Phosphocholine (98%)	Lipoid	511980-1180002/904
Ethanol	Sigma-Aldrich	32221
Methanol	Sigma-Aldrich	34885

Chloroform	Merck	S5617420 334
Glutaraldehyde	Sigma-Aldrich	S8052503 052
Ammonium sulfate	Merck	7783-20-2
Paraformaldehyde	CARLO ERBA	387507
Hydrochloric acid	Merck	K41078514 018

2.4.2 Protocols of Liposome Experiments

2.4.2.1 Liposome Production

Lipids were mixed 1:1 in mass in methanol and chloroform, and were processed in the rotary evaporator until fully evaporated to form a lipid thin film on glass flask surface. The resultant film was rehydrated with 300nM ammonium sulfate buffer and mixed vigorously on vortex. For size homogenization of liposomes, they were subjected to ultrasonication with 30% power for 1 minute, three cycles with 10 minutes resting time in-between. After production, in order to secure a saline environment outside the liposomes, they were then dialyzed against PBS for 2 hours using a 1kDa dialysis membrane.

2.4.2.2 Size Characterization of Liposomes by Dynamic Light Scattering

Measurement was conducted using disposable microcuvettes which were cleaned with distilled water and air-dried before use. All the measurements were performed in triplicates at defined parameters, by adding viscosity and refractive index information at room temperature. To obtain the average hydrodynamic diameter and polydispersity index (indicates width of size dispersion), cumulative analysis algorithm was applied.

2.4.2.3 Morphological Characterization of Liposomes by Scanning Electron Microscope

The liposome sample was spread on a clean and dry cell culture plate surface and air-dried overnight in the fume hood. Then it was incubated at 4°C overnight, immersed in 4% glutaraldehyde in PBS. After it was air-dried in the fume hood for a few hours, it was mounted on a stub with a carbon-conductive adhesive tape, and sputtered in a vacuum with 10nm thickness gold and palladium. It was analyzed on SEM with a field emission gun (FEG-SEM) operated in a high vacuum environmental mode, at 30.0 kV accelerating voltage.

2.4.2.4 Resiquimod Encapsulation by Liposomes

A total of 628 μM stock of resiquimod in DMSO was dissolved in 1mL of distilled water with hydrochloric acid (pH2.5), to protonate the drug, for 1 hour at room temperature. After protonation, the solution was introduced to 3 mL of liposomes, which were size-homogenized and dialyzed against PBS. The resulting solution was mildly mixed for 1 hour at 45°C, and were then dialyzed against PBS for 2 hours using a 1kDa dialysis membrane to eliminate non-encapsulated resiquimod molecules. After dialysis, resiquimod-encapsulated liposomes were ready for characterization or treatment, and were kept at 4°C for a maximum time of 1 week. Liposomes were filtered through PFTE membrane (0.22μm) before cell treatment.

2.4.2.5 Quantification of Liposome-Encapsulated Resiquimod by Quadrupole Time-of-Flight Mass Spectroscopy (qTOF-MS)

The spectroscope equipped with a binary pump, an online degasser, an autosampler and a thermostated column compartment coupled with a 6540 Q-TOF-MS with a Dual ESI source (Agilent Technologies, Santa Clara, CA, USA) was utilized. ESI source

was operated in positive and negative ion modes, where the fragmentor voltage was 120V, nebulizer gas was 35psig, capillary voltage was 3500V, drying gas flow rate was 10dm^3/min, and drying gas temperature was 300°C. The mobile phase (0.01% formic acid in water) flow rate was 0.5 cm^3/min and the injection volume was 10mm^3. Collision energy ramp with a range of 15-40eV was use to promote fragmentation for MS/MS measurements. Data was acquired using High Resolution mode with 4GHz, and the mass range was set at 50-1000m/z. MassHunter Workstation Qualitative Analysis B.03.01 Software was used to process the data.

2.4.2.6 Liposome Phagocytosis Assay

3mM Nile Red was prepared in 1:10 DMSO:ethanol mixture as a stock solution. Liposomes were incubated overnight with Nile Red working concentration of 3μM at RT. The solution was dialyzed against 1kDa dialysis membrane to remove unbound dye molecules. TAM-transformed THP-1 macrophages and HT-29 cells were treated with Nile Red-stained liposome working concentration of 3μM for 1 day. The cells were washed with PBS to be observed on the fluorescence microscope, after staining with F-actin and DAPI.

Chapter 3

Results

3.1 Resiquimod-Loaded Liposome Characterization

In the study, liposomes were produced by lipid thin film hydration method, and were subjected to ultrasonication for size homogenization, before drug loading and phagocytosis assays (see Figure 6). Upon hydration of the lipid thin film, the size distribution on DLS revealed a highly heterogeneous profile with a polydispersity index of 1.00 as expected. Because sizes smaller than 100nm are much more prone to phagocytosis by non-phagocytic cells, we opted for a size range of 150-1000nm with lower than 0.30 polydispersity index. When these liposomes were treated with the optimized parameters of ultrasonication, average size was fixed at around 170-200nm, with a polydispersity index reduced to 0.23.

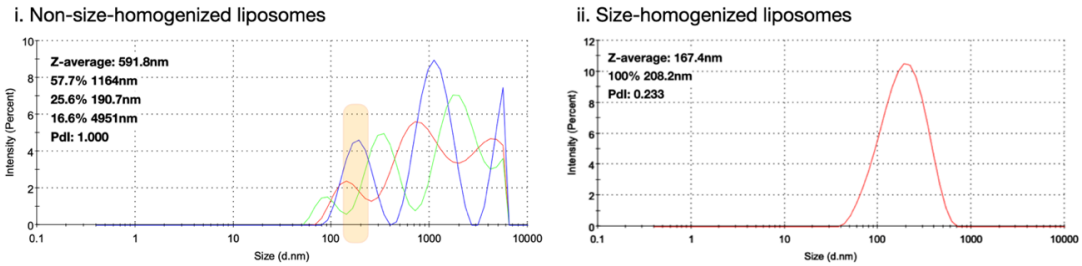

Figure 6. Size distribution of non-size-homogenized (i) and ultasonication-based size-homogenized liposomes (ii) by DLS analysis. Size homogenization seems to shift most liposomes to the emphasized peak (in i).

SEM analysis of the liposomes proved such size homogenization as well, besides morphologically revealing their enclosed, circular structure (Figure 7).

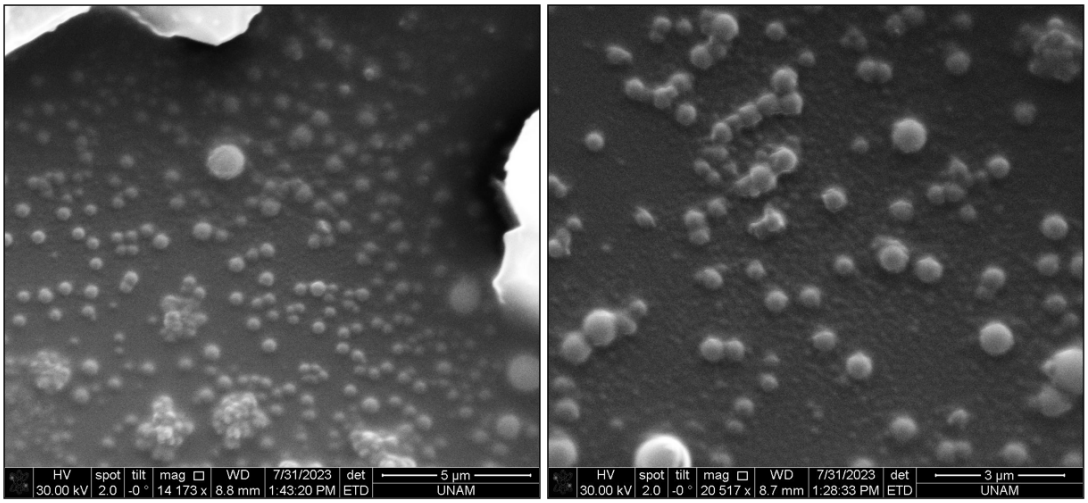

Figure 7. SEM images of the size-homogenized liposomes. DLS results seem to be validated in microscopic observation as well, besides showing a targeted spherical morphology.

Even though they were only treated to THP-1 cells in this study, one motivation of liposomal encapsulation of the drug was targeting the phagocytic abilities of macrophages in a later *in vivo* application. Therefore, before drug encapsulation, the produced liposomes were tested for the selectiveness of their phagocytosis. After liposome labeling with the lipophilic dye Nile Red (Figure 8), THP-1 and HT-29 cells were treated with the labeled liposomes, and were analyzed by tracking the localization of the dye with respect to F-actin and nucleus (Figure 9). Compared with the negative control where the dye was provided to the cells directly, liposome-bound Nile Red was detected closer to the nuclei and co-localized with F-actin for THP-1 cells, suggesting internalization of the liposomes by these cells. In HT-29 cells, as expected, no such difference was observed.

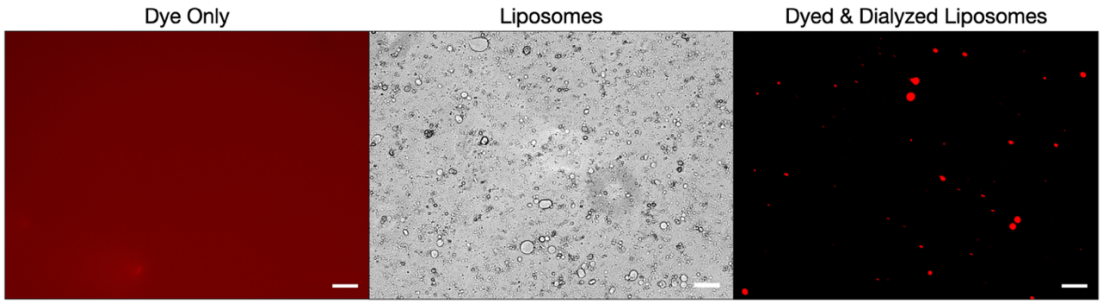

Figure 8. Fluorescence and bright observation of dye and liposomes alone, as well as dye-incubated and dialyzed liposomes, to show for labeling of liposomes. Scale bars: 200μm for dye and liposome samples, 50μm for dyed and dialyzed liposomes.

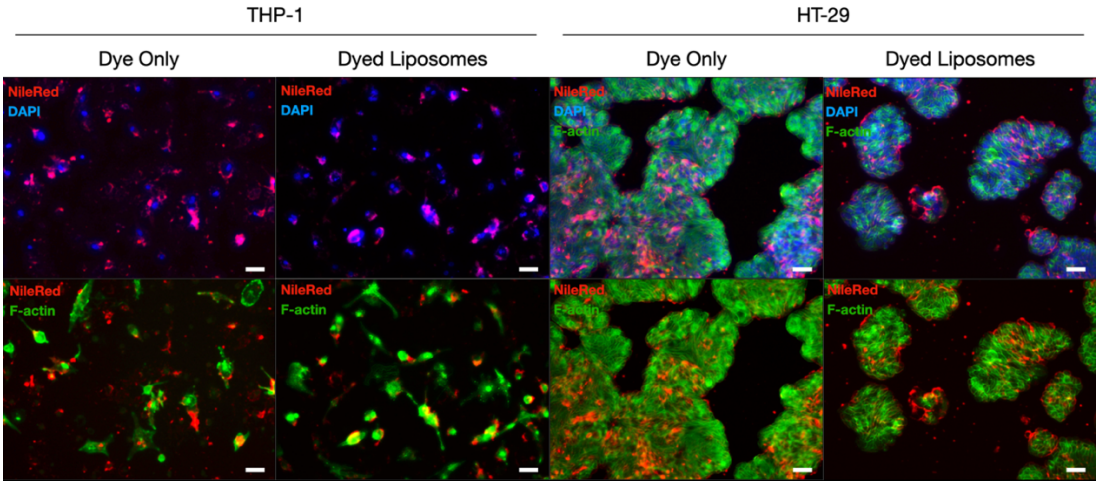

Figure 9. Phagocytosis assay of liposomes by THP-1 macrophages (in tumor-associated polarization) and HT-29 cells. Scale bars: 50μm.

As for the liposomal encapsulation of resiquimod, the efficiency of remote loading was calculated by the below formula (Equation 1), which compares intensities of resiquimod-only and lysed sample of resiquimod-encapsulating liposomes in qTOF-MS analysis.

Equation 1. Formula for drug encapsulation efficiency calculation by analysis of intensity values depicted in qTOF-MS.

$$\frac{\text{Drug peak intensity for liposome solution}}{\text{Drug peak intensity for drug only solution}} \times \frac{\text{Drug concentration in drug only solution}}{\text{Drug concentration in liposome solution}} \times 100\%$$

The analysis report revealed the presence of resiquimod (MW: 314) in both solutions (Figure 10). With a free resiquimod concentration of 157µg/mL, we have obtained a peak with the intensity of 7,092,355. Meanwhile, for the final liposome solution that had completed all the steps up to the last dialysis and was lysed to leash the encapsulated resiquimod, the concentration of resiquimod used for remote loading after dilutions for spectroscopic analysis was 60.58µg/mL, which yielded a peak with the intensity of 2,634,230. The calculations below were then followed (Equation 2), to find the encapsulation efficiency.

i. qTOF-MS of free resiquimod

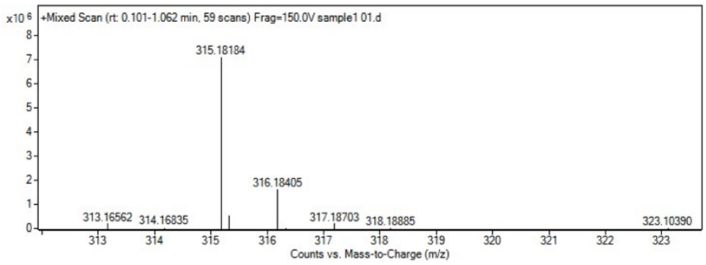

ii. qTOF-MS of lysed resiquimod-encapsulated liposomes

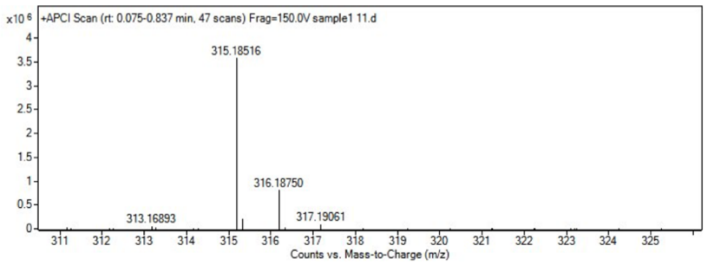

Figure 10. Spectra found by qTOF-MS analysis of free resiquimod (i) and lysed resiquimod-encapsulated liposomes (ii). With a molecular weight of 314, resiquimod shows a clear peak with a hydrogen-bound form in the analysis, at a total molecular weight of 315. The intensity values of the peaks were analyzed by the software as 7,092,355 (i) and 2,634,230 (ii).

Equation 2. Encapsulation efficiency calculation for resiquimod-encapsulated liposomes, using intensity values of the peaks in qTOF-MS analysis.

$$\frac{2{,}634{,}230}{7{,}092{,}355} \times \frac{157\mu g/mL}{60.58\mu g/mL} \times 100\% = \mathbf{96.26\%}$$

Hence, a set of physicochemical and biophysical characterizations had drawn us to the conclusion, that the liposomes produced with our optimized protocol were sized around 200nm with an acceptable polydispersity index, could encapsulate resiquimod with 96.26% efficiency, and were readily phagocytosed by THP-1 cells but not by HT-29 cells.

3.2 Transformation of THP-1 Macrophages into Tumor-Associated Polarization

Macrophages are highly plastic cells, and once activated, they are able to change their phenotype and thus function accordingly to the stimuli they are exposed to in their environment. Activated macrophages are usually classified as either M1-like polarization, which is associated with pro-inflammatory response with active roles in fighting infections and activating further immune response, and an anti-inflammatory M2-like polarization(Yunna et al., 2020). M1 state inhibits cell proliferation, increases tissue damage, mediate immune response of other immune cells; whereas M2 state activity promotes cell proliferation, tissue repair, resolution of inflammation(Mills, 2012; Yunna et al., 2020). Though these suggest for a switch mechanism, there is usually a mixture of both functions present in an environment, and especially with tumor-associated polarization which is a so-called state for tumor-infiltrating macrophages, macrophages with mixed and heterogeneous M1-like and M2-like polarizations are implied. They are found to be involved in producing an immune-suppressive tumor microenvironment, enhance angiogenesis, induce epithelial-to-mesenchymal transition and proliferation of cancer cells, mediate countless cell-to-cell interactions to secure a tumor-accommodable environment, and wire the extracellular matrix (Yang et al., 2020). Thus, we opted for a comprehensive set of characterizations to assess the transformation.

In this work, because of the relevant findings in literature, we first assessed the transformation by analyzing bright-field images of macrophages (Figure 11), as the activated state of macrophages are implied with a change in morphology, with a more spread cell attachment (Deng et al., 2021; Y. Huang et al., 2019; Wheeler et al., 2018; Xu et al., 2018) and an increased production of extracellular vesicles (Cianciaruso et al., 2019; Lu et al., 2021). We have detected a significant difference between THP-1 macrophages and their HT-29-conditioned media incubated states, especially in production of extracellular vesicles and general appearance of the cells, where

cellular borders became a bit vaguer, and cells became more spread in the transformed state.

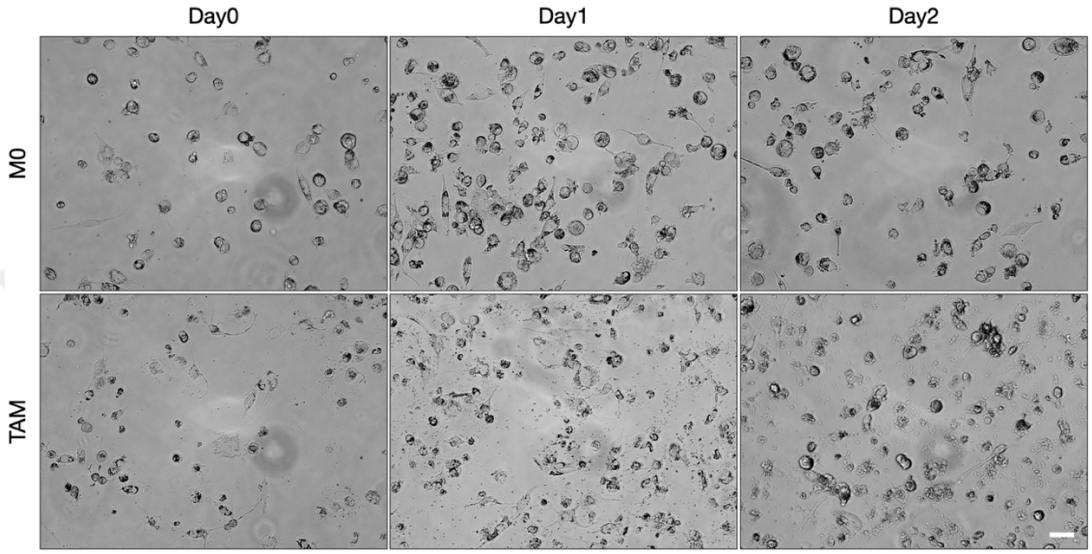

Figure 11. Bright-field analysis of non-transformed (M0) and HT-29-conditioned media treated macrophages (TAM) on three consecutive days. Scale bar: 50μm.

To further test the spreading features, where M2-like tumor-associated state was expected to have a smaller minor to major axis ratio, we used F-actin staining which validated a change in axial conformations of the macrophages after HT-29-conditioned media incubation (Figure 12).

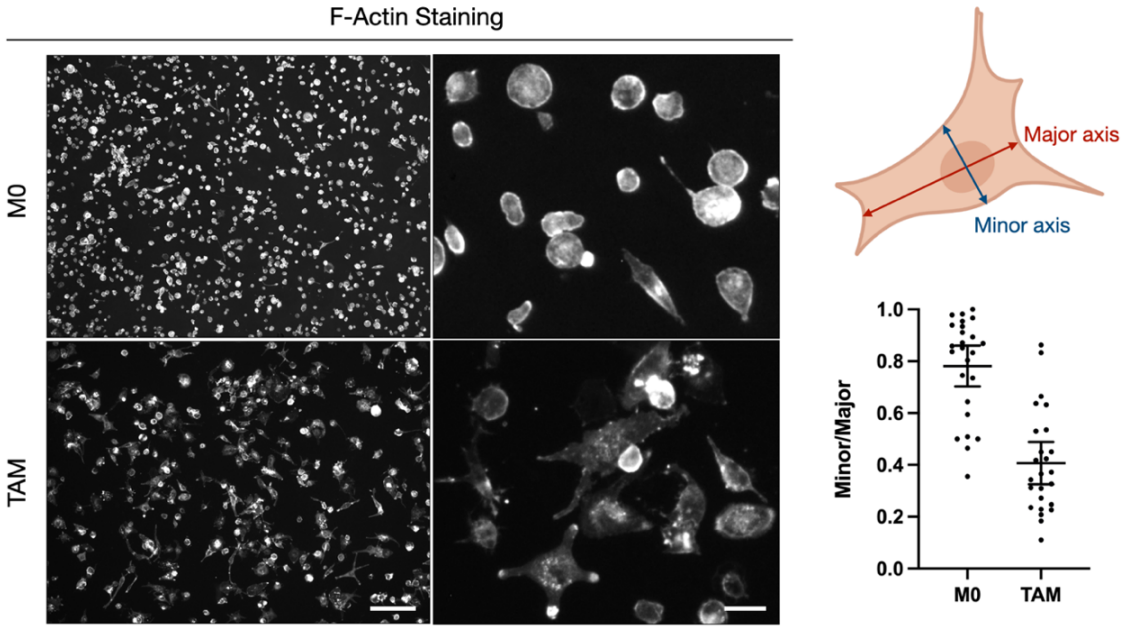

Figure 12. Analysis of cytoplasmic spread of non-transformed (M0) and HT-29-conditioned media treated macrophages (TAM). Scale bar for far-images is 100μm, for close-up views is 20μm. Minor axis to major axis ratios were collected for 25 random cells. Error bars indicate 95% confidence interval.

Despite morphological heterogeneity of M1 and M2 marker expressions, tumor-associated macrophages are thus often categorized as M2-like polarization states, and thus are often assessed by the ratio of M1 to M2 marker expressions. We analyzed M1 marker of CD86 and M2 marker of CD163 on THP-1 tumor-associated macrophages, by flow cytometry (Figure 13) and immunocytochemistry (Figure 14). Interestingly, all cells in both non-transformed and HT-29-conditioned media treated macrophages were CD163+ as found by flow cytometry, yet immunocytochemistry showed for a clear difference in fluorescence intensities; suggesting an absence of complete halting, yet a substantial decrease, of CD163 expression in HT-29-conditioned media treated macrophages compared to non-treated ones. For CD86, a similar pattern was observed for both characterization techniques, where both the ratio of CD86+ cells were reduced to half, and the fluorescence intensity of the

receptor was substantially reduced in immunocytochemistry analysis, through HT-29-conditioned media treatment.

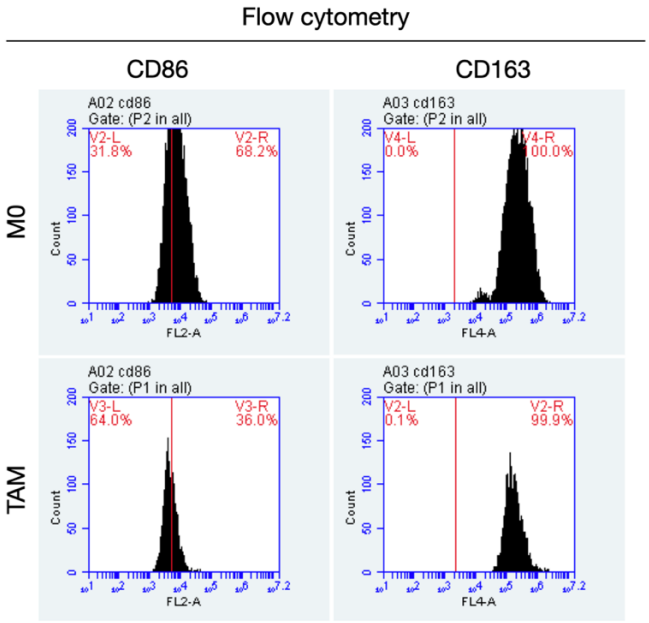

Figure 13. Flow cytometry analysis to detect CD86+ and CD163+ macrophage populations of non-transformed (M0) and HT-29-conditioned media treated macrophages (TAM).

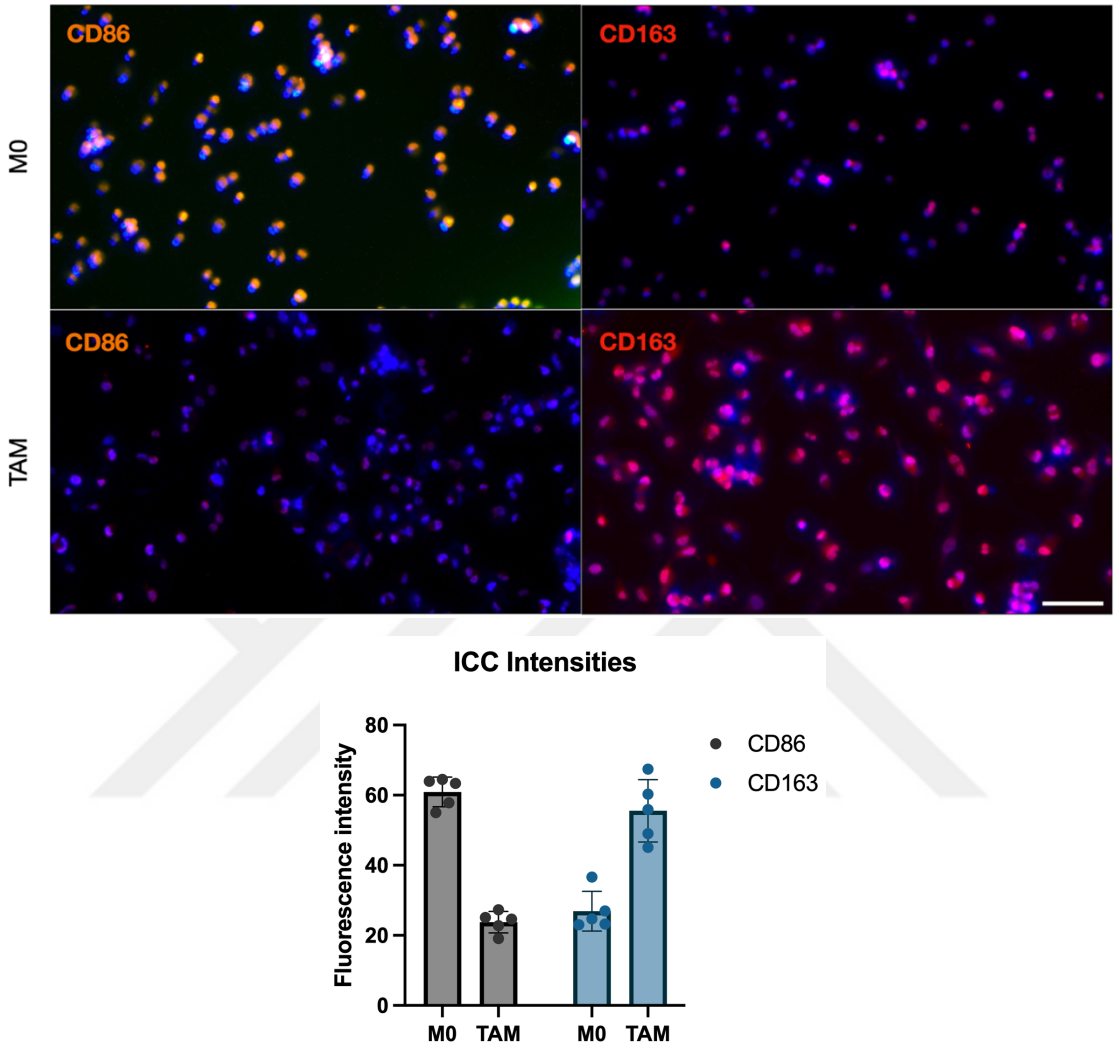

Figure 14. Immunocytochemistry for CD86 and CD163 receptors on non-transformed (M0) and HT-29-conditioned media treated macrophages (TAM). Scale bar: 100μm. Fluorescence intensities are quantified for five random cells in each population.

Overall, we concluded that HT-29-conditioned media incubation, as suggested in literature (Wei et al., 2019), was able to transform THP-1 macrophages into tumor-associated macrophages.

3.3 Re-Education of Tumor-Associated Macrophages by Resiquimod-Encapsulating Liposomes

In this section, we first analyzed the success of re-education by resiquimod-encapsulating liposomes, by comparing with resiquimod-only treatments, for CD86+ cell ratios and fluorescence intensities of immunocytochemistry for CD163; as well as morphological assessment. After showing that liposome-encapsulation of resiquimod did not reduce the capability of the molecule to impact tumor-associated THP-1 macrophages, we continued by re-educating by resiquimod-encapsulating liposomes and analyzing the impact of re-education, by comparing how tumor-associated THP-1 macrophage-conditioned versus re-educated tumor-associated THP-1 macrophage-conditioned media incubation of HT-29 cells affected cancer cell morphology, proliferation (by coverage assay), spheroid growth, metastatic capabilities (by wound healing assay), and stemness (by immunocytochemistry for CD133).

In terms of bright-field morphological observations, there were no apparent difference detected amongst tumor-associated macrophages, free resiquimod treated tumor-associated macrophages, free liposome treated tumor-associated macrophages, and resiquimod-encapsulating liposome treated tumor-associated macrophages (Figure 15). Nevertheless, staining F-actin and nucleus revealed a more spread morphology in both free resiquimod treated and resiquimod-encapsulating liposome treated ones (Figure 15). We also detected that some cells had multiple nuclei after resiquimod-encapsulating liposome treatment (Figure 15); which has been associated with Interleukin-4 and Interleukin-13-dependent macrophage fusion to yield multinucleated giant cells (McNally & Anderson, 2011), which is a phenotype also shown in tumor-associated state of macrophages in solid tumor sections (Caillou et al., 2011).

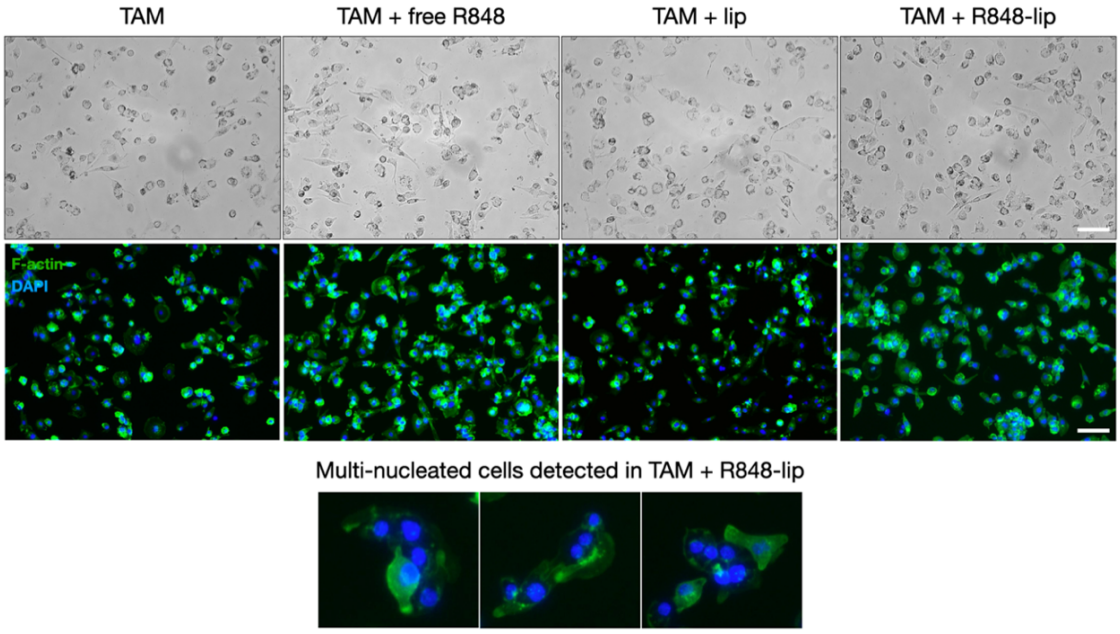

Figure 15. Bright-field and F-actin with DAPI staining for morphological assessment of treatments done on tumor-associated macrophages (TAMs): free resiquimod (TAM + free R848), free liposome (TAM + lip), resiquimod-encapsulating liposome (TAM + R848-lip). Scale bars: 100μm.

Immunocytochemistry for CD163 revealed that the expression of the marker for M2-like polarization state was substantially reduced in free resiquimod and resiquimod-encapsulating liposome treatments, but not in free liposome treatment (Figure 16).

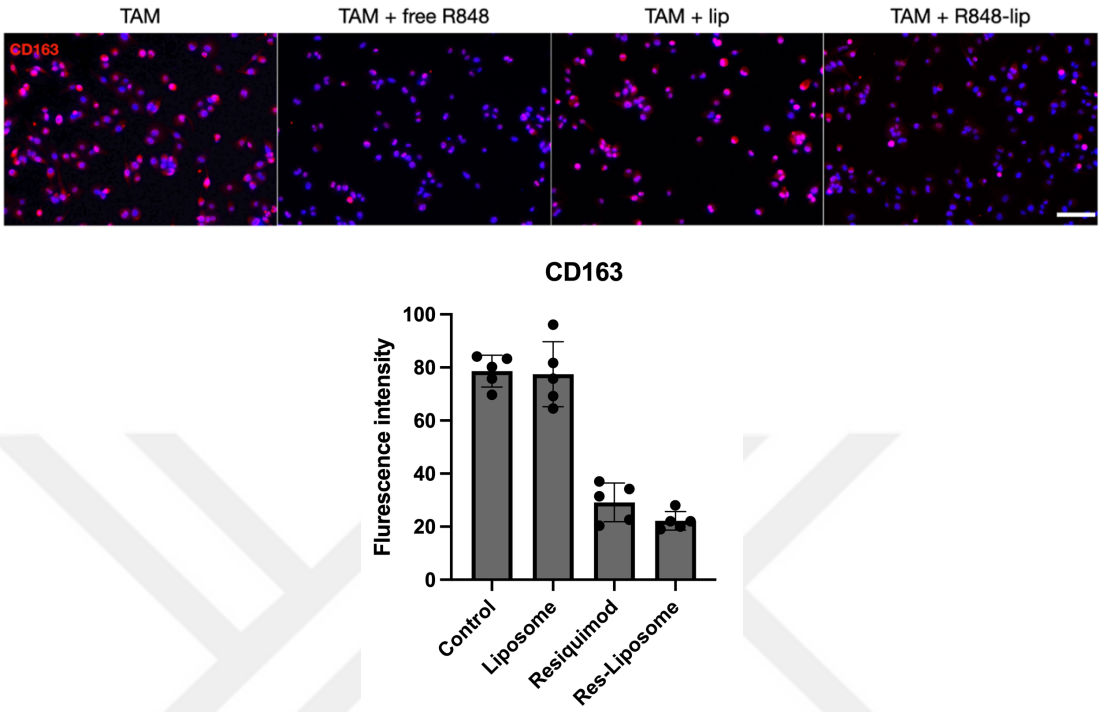

Figure 16. CD163 immunocytochemistry analysis for morphological assessment of treatments done on tumor-associated macrophages (TAMs): free resiquimod (TAM + free R848), free liposome (TAM + lip), resiquimod-encapsulating liposome (TAM + R848-lip). Scale bar: 100μm. Fluorescence intensities are quantified for five random cells in each population.

As the re-education by resiquimod-encapsulating liposomes was validated, we passed to investigate the reaction of HT-29 cells to the re-education. On an interesting note, HT-29 cells were changed from DMEM culture to RPMI 1640 culture for this study, which not only facilitated conditioned media incubations, but also was significant in terms of the maturation state of HT-29 cells; as in DMEM, 1-methyl-tryptophan inhibits 2,3 dioxygenase-1 (the initial enzyme in tryptophan metabolism along the kynurenine pathway) and therefore prevents goblet cell differentiation, whereas tryptophan and kynurenine present in RPMI 1640 induces goblet cell differentiation shown by activated Notch1 and reduced β-catenin expression (Park et al., 2018). The difference in morphology at full confluency suggested increased

maturation with villi formation (Figure 17), when compared to literature (Hekmati et al., 1990), though we did not characterize the formation of these villi in this work.

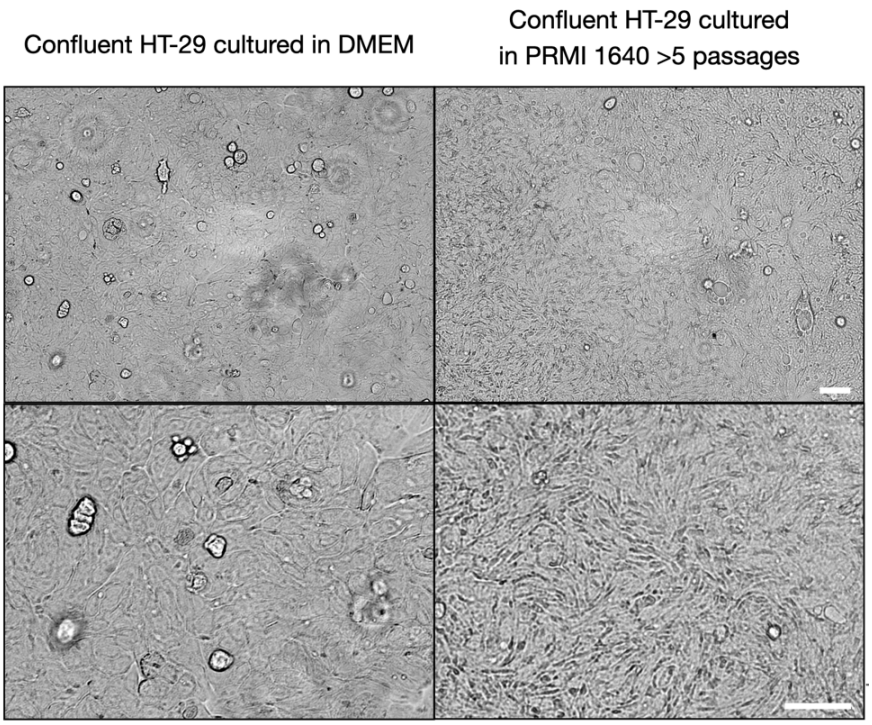

Figure 17. Bright-field images of confluent HT-29 cells cultured in DMEM and confluent HT-29 cells cultured in RPMI 1640 for more than 5 passages. Scale bars: 50µm.

The treatments of re-educated tumor-associated THP-1 macrophage-conditioned media and tumor-associated THP-1 macrophage-conditioned media on HT-29 cells were first characterized by their impact on HT-29 morphology (Figure 18). A substantial difference was observed, where the tumor-associated macrophages seemed to exert a mesenchymal-transition-inducing impact on the cancer cells, characterized by transformation into a more stretched morphology. Re-education was seemingly unable to halt this effect to the full, though the level of induction was observed to be reduced.

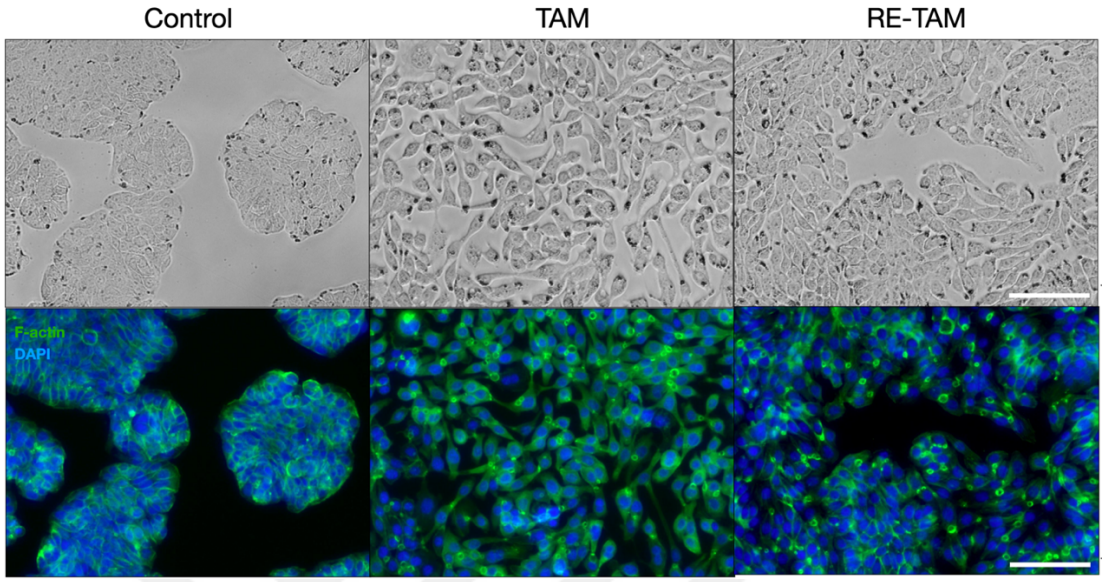

Figure 18. Bright-field and respective F-Actin and DAPI staining analyses of HT-29 cells incubated with RPMI 1640 (Control), tumor-associated THP-1-conditioned media (TAM), and re-educated tumor-associated THP-1 conditioned media (where re-education was mediated by resiquimod-encapsulating liposomes) (RE-TAM). Scale bars: 100μm.

The proliferation rates of HT-29 cells on the treatments were analyzed by a coverage assay (Figure 19). A clear increase in proliferation was evident in tumor-associated macrophage-conditioned media treatment, where the confluency reached from around 40% to around 90% after one day. Re-education was found to lighten this extreme impact, yet couldn't reverse it to the level of negative control.

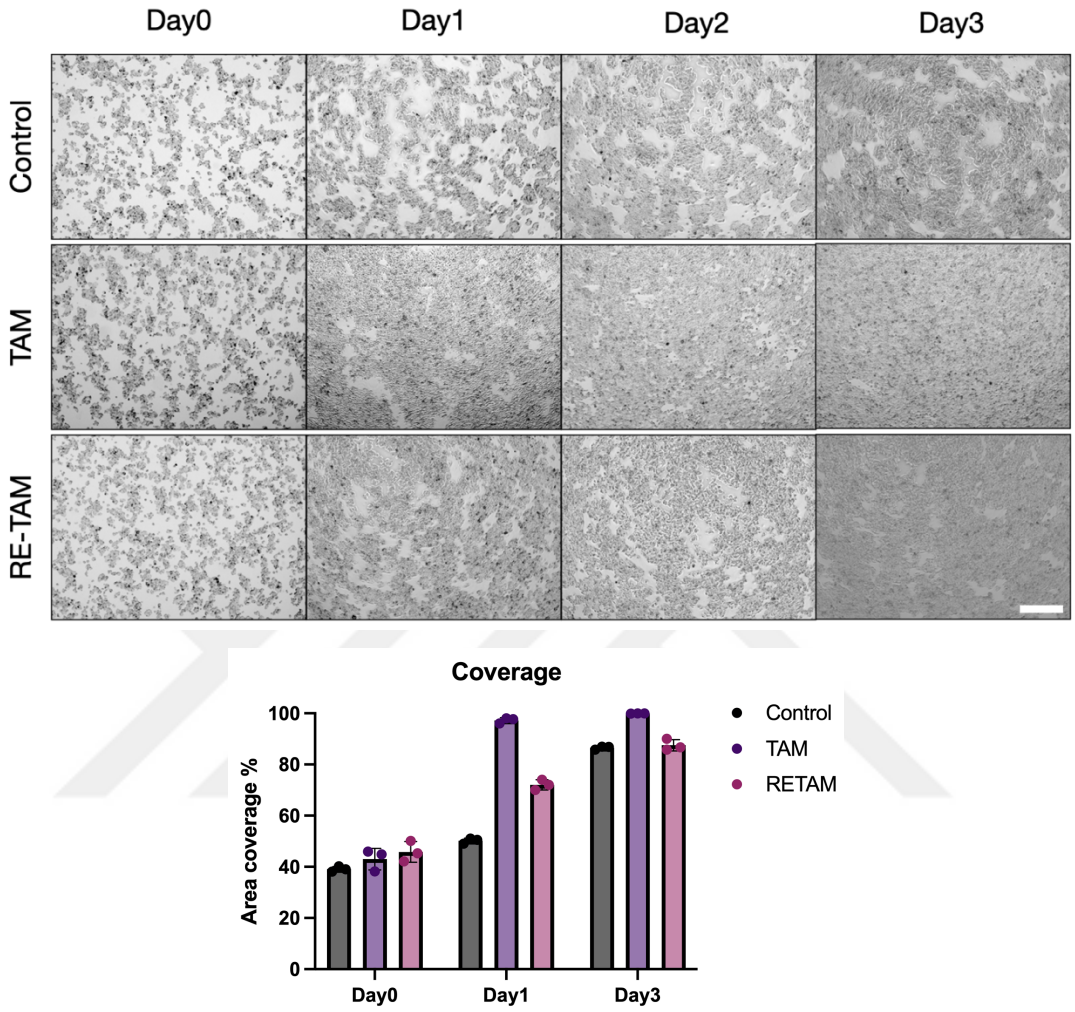

Figure 19. Coverage assay analysis of HT-29 cells incubated with RPMI 1640 (Control), tumor-associated THP-1-conditioned media (TAM), and re-educated tumor-associated THP-1 conditioned media (where re-education was mediated by resiquimod-encapsulating liposomes) (RE-TAM). Scale bar: 500µm. Percent covered areas are quantified for 3 cases for each treatment.

As assessed by flow cytometry, the impact of re-education on HT-29 viability showed a similar impact as proliferation analysis, where tumor-associated THP-1 conditioned-media treatment reduced dead cell ratio from 28% to 5%, and re-education only could increase it back to around 12% (Figure 20).

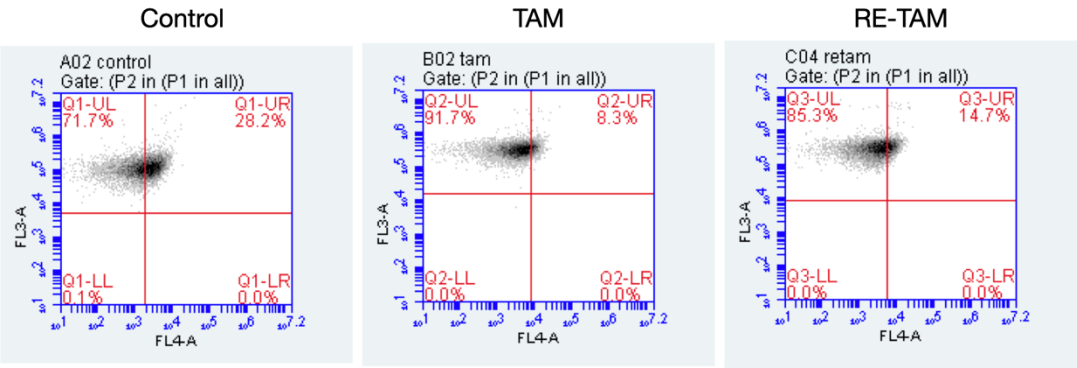

Figure 20. Flow cytometry analysis to detect dead (Q1) and viable cells (Q4) in HT-29 cells incubated with RPMI 1640 (Control), tumor-associated THP-1-conditioned media (TAM), and re-educated tumor-associated THP-1 conditioned media (where re-education was mediated by resiquimod-encapsulating liposomes) (RE-TAM).

As another growth assessment, HT-29 spheroid growth profiles under the treatments were also analyzed (Figure 21). In the assay, tumor-associated THP-1 macrophages were shown to increase the growth rate of the three-dimensional culture of cancer cells, whereas re-education was implied a rescue of the impact, causing similar growth profiles as control spheroids.

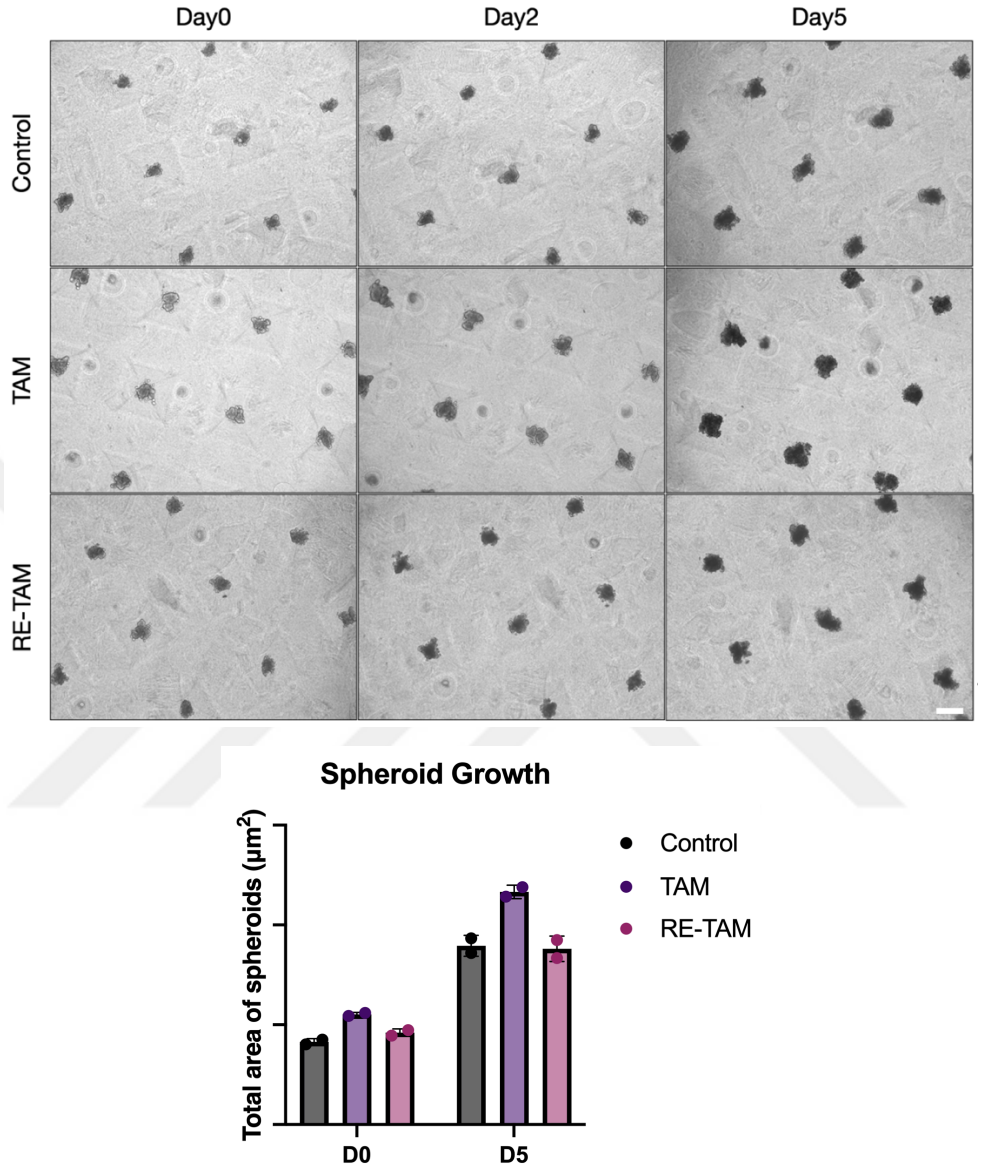

Figure 21. Growth analysis HT-29 spheroids incubated with RPMI 1640 (Control), tumor-associated THP-1-conditioned media (TAM), and re-educated tumor-associated THP-1 conditioned media (where re-education was mediated by resiquimod-encapsulating liposomes) (RE-TAM). Scale bar: 500µm. Percent covered areas are quantified for averaging 20 spheroids for two times of treatments.

Next, migrative capabilities of HT-29 cells were analyzed under treatments (Figure 22). The wound-healing assay confirmed the hypothesis that the migration would be

enhanced under tumor-associated THP-1 macrophage conditioned-media, which was also supported by the mesenchymal-like transformation depicted in morphological analyses (Figure 18). Re-education seemed to completely reverse the migration-inductive impact of tumor-associated macrophages, and furthermore, the treatment yielded with less migration of HT-29 cells as compared to control.

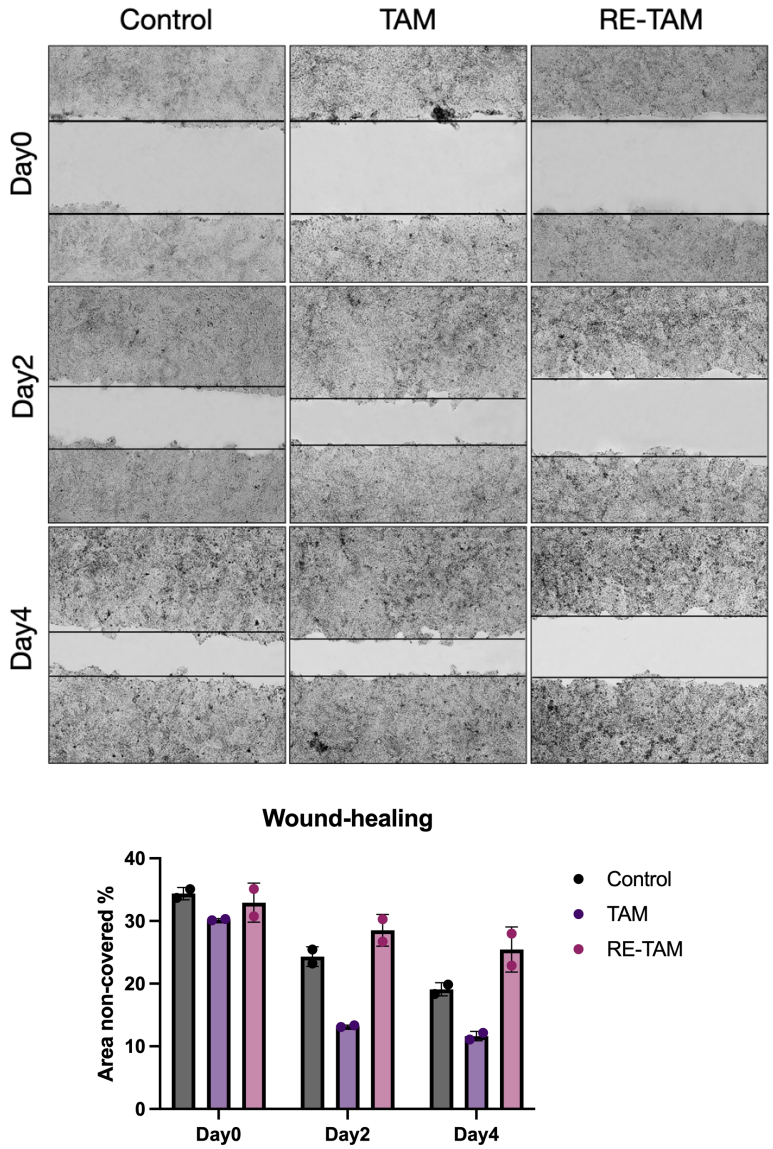

Figure 22. Wound-healing analysis of HT-29 cells incubated with RPMI 1640 (Control), tumor-associated THP-1-conditioned media (TAM), and re-educated

tumor-associated THP-1 conditioned media (where re-education was mediated by resiquimod-encapsulating liposomes) (RE-TAM). Non-covered area percentages are quantified for two replicates of each treatment.

Finally, we analyzed the change in stemness of HT-29 cells under treatments, by immunocytochemistry for CD133 (Figure 23), which is a well-described cancer stem cell marker present in various colorectal carcinoma cell lines, including HT-29 (WANG et al., 2012). The expectation of tumor-associated macrophages increasing the expression of CD133 was confirmed by the analysis. Re-education was shown to reduce stemness according to the results, though not to the extent of control.

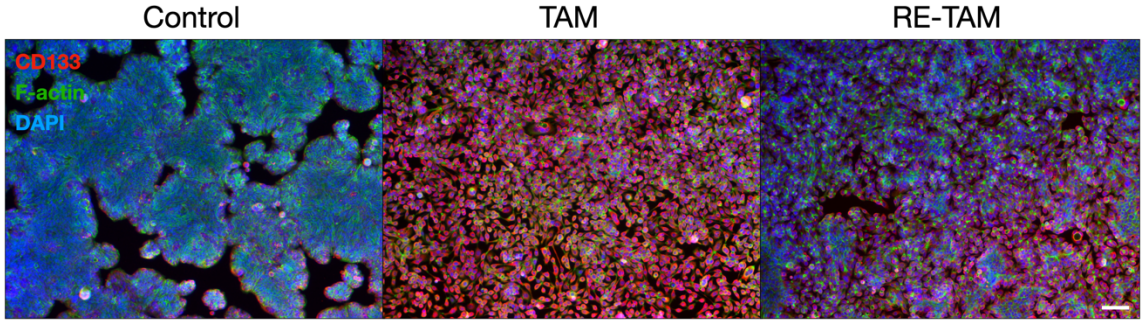

Figure 23. Fluorescence images of immunocytochemistry for CD133 complemented with F-actin and DAPI staining of HT-29 cells incubated with RPMI 1640 (Control), tumor-associated THP-1-conditioned media (TAM), and re-educated tumor-associated THP-1 conditioned media (where re-education was mediated by resiquimod-encapsulating liposomes) (RE-TAM). Scale bar: 100μm.

Chapter 4

Discussion and Future Perspective

Immunotherapy, despite inheriting an obvious complexity and uncertainty, offers a great therapeutic promise especially over single-handed traditional cytotoxic therapies for cancer. Combinatorial approaches of immunotherapies with chemotherapies (Ning et al., 2021; Padrón et al., 2022; Sjoquist, 2023) and radiotherapies (Romano et al., 2021) that made it to clinical trials have yielded with extremely promising (Barbari et al., 2020; Zhu et al., 2021), yet often controversial conclusions so far for various kinds and stages of cancer (Q. Chen et al., 2022), usually because of the high rate of adverse reactions by overly activated immune components. Targeting and controlling the immune attack, as well as optimizing efficiency in any kind of treatment strategy, is arguably best addressed by analyzing the tumor microenvironment and taking its most therapy-influential features into consideration.

In this thesis, we targeted an indispensable helper of cancer cells in any solid tumor microenvironment, that is tumor-associated macrophages, and aimed to reverse their tumor-helping functions by providing a strong immune activator of TLR7/8 agonist, resiquimod, in a liposome. Liposomal encapsulation was strategized to enhance targeted delivery of the agonist to the solid tumor site, benefiting from enhanced permeability and retention effect, as well as size-dependent selective phagocytosis by macrophages.

There are a few discussion points on the obtained observations, perhaps the biggest one being the naming of the transformed macrophages as tumor-associated macrophages, while there weren't enough characterization steps followed to confirm their tumor-associated state. Therefore, we'd like to declare here that what we meant throughout the thesis by tumor-associated macrophages, was actually only HT-29-conditioned media treated THP-1 macrophages, of which we showed some extend of results for inclination towards an M2-like polarization. One other questionable factor is the more maturated state of HT-29 cells because of using RPMI1640 medium instead of DMEM. The impact of such maturation on the malignant properties of cells was not assessed in this work, and therefore if it causes some kind of loss of the cancerous nature of the cells, the results might be misleading in the way of clinical translation. The proposed advantages for utilizing liposomes as carriers for resiquimod, which speculated to be tumor-site accumulation due to the enhanced permeability and retention effect, as well as reduced systemic inflammation with selective phagocytosis by phagocytic cells, were not validated in this study, therefore it could be ideal to detect the infiltration of the liposomes into solid tumors through distorted vessels around the tumor microenvironment, and a comprehensive analysis of the inflammation states throughout the whole body would be desperately needed in carrying this work to upper levels.

In the current state of the work, with the designed and well-characterized liposomes, we obtained some promising preliminary in vitro data on the reversal of cancer-helping impacts of tumor-associated macrophages through re-education. The cell proliferation rates, which was more physiologically-relevantly assessed by spheroid growth assay, showed a clear decline after re-education. Increased morphological epithelial-to-mesenchymal transition cues under the tumor-associated macrophage influence were also validated by wound-healing assay, where re-education impact was again visible. We have also observed an increase in stemness through tumor-associated macrophage help, which was reduced upon re-education, yet because of

the assays done to assess the stemness were futile, the promising results in this particular function need to be validated much further, especially because of the vastly differential components of the stemness of cancer stem cells. This was generally a serious limitation of the whole work, the variety of assays and the number of repeat experiments, yet a certain direction was still obtained, towards a successful re-education of tumor-associated cells with the proposed strategy.

Even though the success of our strategy was not completely assessed in the current state of the study, it keeps the potential for future studies, where other non-cancerous cell types and/or tumor-induced endothelial components could also be included to prove for the advantage of liposomal encapsulation. Besides model animals, microphysiological systems are also great candidates for such further testing. In that case, the liposome construct could be modified as well, for example by increasing stability via including cholesterol in the lipid bilayer. Once the functionality of the resiquimod-encapsulating liposomes we observed in this study is more sophistically validated, the carrier system also inherently bears some potential for further functionalization, such as surface-modification on lipid membrane of the liposomes. Hence, various kinds of molecule-based therapies, including chemotherapeutic ones, could be implemented in the liposomal construct, without inhibiting the immune-activating functions.

All these advantages coming with utilizing liposomes as drug carriers are already well-recognized and appreciated, and there are other works in the literature in which resiquimod-encapsulated liposomes were treated on tumor-associated macrophages (H. Li et al., 2021; Pauli et al., 2021). What this study further offers is basically an examination of the impact those works also concluded, yet this time on in vitro transformed tumor-associated THP-1 macrophages with the colorectal adenocarcinoma cell line HT-29. In certain consensus molecular subtypes of colorectal cancer based on tumor gene expression profiles, namely subtype 2

(canonical) and subtype 3 (metabolic) where the immune and stromal infiltration is very low, enhancing the immunogenicity of tumor microenvironment is proved to be a well-working treatment strategy (Colangelo et al., 2017). The epithelial goblet cell line HT-29 is characterized to belong to subtype 3 (Miller et al., 2021), where metabolic imbalances that are often associated with hypermutations and microsatellite instability are hold responsible from the initiation of malignant phenotype; therefore, testing the efficiency of an immunogenicity-increasing treatment strategy on these cells, we aimed to get in vitro results that may be relevant in the clinic for colorectal cancer with consensus molecular subtype 3 cases.

Overall, in this thesis, an immunotherapeutic approach of liposomal TLR7/8 agonist treatment on tumor-associated macrophages in colorectal cancer was explored in vitro. Using THP-1 and HT-29 cell lines, which were selected to bear a potential of clinical translatability for future research, we concluded that the liposomes re-educated tumor-associated macrophages, and that the re-education reversed their positive impact on stemness, metastatic capabilities, and growth of colorectal cancer cells.

Bibliography

Abbasi, H., Rahbar, N., Kouchak, M., Khalil Dezfuli, P., & Handali, S. (2022). Functionalized liposomes as drug nanocarriers for active targeted cancer therapy: a systematic review. In *Journal of Liposome Research* (Vol. 32, Issue 2, pp. 195–210). Taylor and Francis Ltd. https://doi.org/10.1080/08982104.2021.1903035

Adams, S. (2009). Toll-like receptor agonists in cancer therapy. In *Immunotherapy* (Vol. 1, Issue 6, pp. 949–964). https://doi.org/10.2217/imt.09.70

Álvarez-Prado, Á. F., Maas, R. R., Soukup, K., Klemm, F., Kornete, M., Krebs, F. S., Zoete, V., Berezowska, S., Brouland, J. P., Hottinger, A. F., Daniel, R. T., Hegi, M. E., & Joyce, J. A. (2023). Immunogenomic analysis of human brain metastases reveals diverse immune landscapes across genetically distinct tumors. *Cell Reports Medicine*, *4*(1). https://doi.org/10.1016/j.xcrm.2022.100900

Anderson, N. M., & Simon, M. C. (2020). The tumor microenvironment. In *Current Biology* (Vol. 30).

Angell, H., & Galon, J. (2013). From the immune contexture to the Immunoscore: The role of prognostic and predictive immune markers in cancer. In *Current Opinion in Immunology* (Vol. 25, Issue 2, pp. 261–267). https://doi.org/10.1016/j.coi.2013.03.004

Baghban, R., Roshangar, L., Jahanban-Esfahlan, R., Seidi, K., Ebrahimi-Kalan, A., Jaymand, M., Kolahian, S., Javaheri, T., & Zare, P. (2020). Tumor microenvironment complexity and therapeutic implications at a glance. In *Cell Communication and Signaling* (Vol. 18, Issue 1). BioMed Central Ltd. https://doi.org/10.1186/s12964-020-0530-4

Barbari, C., Fontaine, T., Parajuli, P., Lamichhane, N., Jakubski, S., Lamichhane, P., & Deshmukh, R. R. (2020). Immunotherapies and combination strategies for immuno-oncology. In *International Journal of Molecular Sciences* (Vol. 21, Issue 14, pp. 1–28). MDPI AG. https://doi.org/10.3390/ijms21145009

Bates, J. P., Derakhshandeh, R., Jones, L., & Webb, T. J. (2018). Mechanisms of immune evasion in breast cancer. *BMC Cancer*, *18*(1). https://doi.org/10.1186/s12885-018-4441-3

Bejarano, L., Jordão, M. J. C., & Joyce, J. A. (2021). Therapeutic targeting of the tumor microenvironment. In *Cancer Discovery* (Vol. 11, Issue 4, pp. 933–959). American Association for Cancer Research Inc. https://doi.org/10.1158/2159-8290.CD-20-1808

Beury, D. W., Parker, K. H., Nyandjo, M., Sinha, P., Carter, K. A., & Ostrand-Rosenberg, S. (2014). Cross-talk among myeloid-derived suppressor cells, macrophages, and tumor cells impacts the inflammatory milieu of solid tumors. *Journal of Leukocyte Biology*, *96*(6), 1109–1118. https://doi.org/10.1189/jlb.3a0414-210r

Bindea, G., Mlecnik, B., Tosolini, M., Kirilovsky, A., Waldner, M., Obenauf, A. C., Angell, H., Fredriksen, T., Lafontaine, L., Berger, A., Bruneval, P., Fridman, W. H., Becker, C., Pagès, F., Speicher, M. R., Trajanoski, Z., & Galon, J. Ô. (2013). Spatiotemporal dynamics of intratumoral immune cells reveal the immune landscape in human cancer. *Immunity*, *39*(4), 782–795. https://doi.org/10.1016/j.immuni.2013.10.003

Blankenstein, T., Coulie, P. G., Gilboa, E., & Jaffee, E. M. (2012). The determinants of tumour immunogenicity. In *Nature Reviews Cancer* (Vol. 12, Issue 4, pp. 307–313). https://doi.org/10.1038/nrc3246

Brahmer, J. R., Tykodi, S. S., Chow, L. Q. M., Hwu, W.-J., Topalian, S. L., Hwu, P., Drake, C. G., Camacho, L. H., Kauh, J., Odunsi, K., Pitot, H. C., Hamid, O., Bhatia, S., Martins, R., Eaton, K., Chen, S., Salay, T. M., Alaparthy, S., Grosso, J. F., … Wigginton, J. M. (2012). Safety and Activity of Anti–PD-L1 Antibody in Patients

with Advanced Cancer. *New England Journal of Medicine*, *366*(26), 2455–2465. https://doi.org/10.1056/nejmoa1200694

Brentjens, R. J., Davila, M. L., Riviere, I., Park, J., Wang, X., Cowell, L. G., Bartido, S., Stefanski, J., Taylor, C., Olszewska, M., Borquez-Ojeda, O., Qu, J., Wasielewska, T., He, Q., Bernal, Y., Rijo, I. V, Hedvat, C., Kobos, R., Curran, K., … Sadelain, M. (2013). *CD19-Targeted T Cells Rapidly Induce Molecular Remissions in Adults with Chemotherapy-Refractory Acute Lymphoblastic Leukemia*. https://www.science.org

Caillou, B., Talbot, M., Weyemi, U., Pioche-Durieu, C., Ghuzlan, A., Bidart, J. M., Chouaib, S., Schlumberger, M., & Dupuy, C. (2011). Tumor-Associated macrophages (TAMs) form an interconnected cellular supportive network in anaplastic thyroid carcinoma. *PLoS ONE*, *6*(7). https://doi.org/10.1371/journal.pone.0022567

Camus, M., Tosolini, M., Mlecnik, B., Pages, F., Kirilovsky, A., Berger, A., Costes, A., Bindea, G., Charoentong, P., Bruneval, P., Trajanoski, Z., Fridman, W. H., & Galon, J. (2009). Coordination of intratumoral immune reaction and human colorectal cancer recurrence. *Cancer Research*, *69*(6), 2685–2693. https://doi.org/10.1158/0008-5472.CAN-08-2654

Cao, Q., Wang, Y., Zheng, D., Sun, Y., Wang, Y., Lee, V. W. S., Zheng, G., Tan, T. K., Ince, J., Alexander, S. I., & Harris, D. C. H. (2010). IL-10/TGF-β-modified macrophages induce regulatory T cells and protect against adriamycin nephrosis. *Journal of the American Society of Nephrology*, *21*(6), 933–942. https://doi.org/10.1681/ASN.2009060592

Chen, Q., Zhang, Z., Li, X., & Bu, L. (2022). Chemotherapy Combined With Immunotherapy as a First-Line Treatment Brings Benefits to Patients With Lung Squamous Cell Carcinoma but Different Risks of Adverse Reactions: A Systematic Review and Meta-Analysis. In *Frontiers in Pharmacology* (Vol. 13). Frontiers Media S.A. https://doi.org/10.3389/fphar.2022.940567

Chen, X., Zhang, Y., & Fu, Y. (2022). The critical role of Toll-like receptor-mediated signaling in cancer immunotherapy. *Medicine in Drug Discovery*, *14*. https://doi.org/10.1016/j.medidd.2022.100122

Cianciaruso, C., Beltraminelli, T., Duval, F., Nassiri, S., Hamelin, R., Mozes, A., Gallart-Ayala, H., Ceada Torres, G., Torchia, B., Ries, C. H., Ivanisevic, J., & De Palma, M. (2019). Molecular Profiling and Functional Analysis of Macrophage-Derived Tumor Extracellular Vesicles. *Cell Reports*, *27*(10), 3062-3080.e11. https://doi.org/10.1016/j.celrep.2019.05.008

Clay, T. M., Custer, M. C., Sachs, J., Hwu, P., Rosenberg, S. A., & Nishimura, M. I. (1999a). Efficient Transfer of a Tumor Antigen-Reactive TCR to Human Peripheral Blood Lymphocytes Confers Anti-Tumor Reactivity. In *The Journal of Immunology* (Vol. 163).

Clay, T. M., Custer, M. C., Sachs, J., Hwu, P., Rosenberg, S. A., & Nishimura, M. I. (1999b). Efficient Transfer of a Tumor Antigen-Reactive TCR to Human Peripheral Blood Lymphocytes Confers Anti-Tumor Reactivity. In *The Journal of Immunology* (Vol. 163).

Colangelo, T., Polcaro, G., Muccillo, L., D'Agostino, G., Rosato, V., Ziccardi, P., Lupo, A., Mazzoccoli, G., Sabatino, L., & Colantuoni, V. (2017). Friend or foe?: The tumour microenvironment dilemma in colorectal cancer. In *Biochimica et Biophysica Acta - Reviews on Cancer* (Vol. 1867, Issue 1, pp. 1–18). Elsevier B.V. https://doi.org/10.1016/j.bbcan.2016.11.001

Cui, L. Y., Chu, S. F., & Chen, N. H. (2020). The role of chemokines and chemokine receptors in multiple sclerosis. In *International Immunopharmacology* (Vol. 83). Elsevier B.V. https://doi.org/10.1016/j.intimp.2020.106314

De Cicco, P., Ercolano, G., & Ianaro, A. (2020). The New Era of Cancer Immunotherapy: Targeting Myeloid-Derived Suppressor Cells to Overcome Immune Evasion. In *Frontiers in Immunology* (Vol. 11). Frontiers Media S.A. https://doi.org/10.3389/fimmu.2020.01680

de Visser, K. E., & Joyce, J. A. (2023). The evolving tumor microenvironment: From cancer initiation to metastatic outgrowth. In *Cancer Cell* (Vol. 41, Issue 3, pp. 374–403). Cell Press. https://doi.org/10.1016/j.ccell.2023.02.016

Deng, Y., Govers, C., Beest, E. ter, van Dijk, A. J., Hettinga, K., & Wichers, H. J. (2021). A THP-1 Cell Line-Based Exploration of Immune Responses Toward Heat-Treated BLG. *Frontiers in Nutrition*, *7*. https://doi.org/10.3389/fnut.2020.612397

Deshpande, P. P., Biswas, S., & Torchilin, V. P. (2013). Current trends in the use of liposomes for tumor targeting. In *Nanomedicine* (Vol. 8, Issue 9, pp. 1509–1528). Future Medicine Ltd. https://doi.org/10.2217/nnm.13.118

Farooq, M., Batool, M., Kim, M. S., & Choi, S. (2021). Toll-Like Receptors as a Therapeutic Target in the Era of Immunotherapies. In *Frontiers in Cell and Developmental Biology* (Vol. 9). Frontiers Media S.A. https://doi.org/10.3389/fcell.2021.756315

Farr, M. A., Joshi, T. P., & Lewis, D. J. (2021). Resiquimod: a new topical immune-response modifier for the treatment of actinic keratosis. In *Expert Opinion on Emerging Drugs* (Vol. 26, Issue 4, pp. 433–434). Taylor and Francis Ltd. https://doi.org/10.1080/14728214.2021.2004694

Fridman, W. H., Pagès, F., Sauts-Fridman, C., & Galon, J. (2012). The immune contexture in human tumours: Impact on clinical outcome. In *Nature Reviews Cancer* (Vol. 12, Issue 4, pp. 298–306). https://doi.org/10.1038/nrc3245

Galluzzi, L., Senovilla, L., Vacchelli, E., Eggermont, A., Fridman, W. H., Galon, J., Sautès-Fridman, C., Tartour, E., Zitvogel, L., & Kroemer, G. (2012). Trial watch: Dendritic cell-based interventions for cancer therapy. In *OncoImmunology* (Vol. 1, Issue 7, pp. 1111–1134). https://doi.org/10.4161/onci.21494

Galon, J., Angell, H. K., Bedognetti, D., & Marincola, F. M. (2013). The Continuum of Cancer Immunosurveillance: Prognostic, Predictive, and Mechanistic Signatures. In *Immunity* (Vol. 39, Issue 1, pp. 11–26). https://doi.org/10.1016/j.immuni.2013.07.008

Galon, J., & Bruni, D. (2019). Approaches to treat immune hot, altered and cold tumours with combination immunotherapies. In *Nature Reviews Drug Discovery* (Vol. 18, Issue 3, pp. 197–218). Nature Publishing Group. https://doi.org/10.1038/s41573-018-0007-y

Galon, J., Costes, A., Sanchez-Cabo, F., Kirilovsky, A., Mlecnik, B., Lagorce-Pagès, C., Tosolini, M., Camus, M., Berger, A., Wind, P., Zinzindohoué, F., Bruneval, P., Cugnenc, P.-H., Trajanoski, Z., Fridman, W.-H., & Pagès, F. (2006). Type, Density, and Location of Immune Cells Within Human Colorectal Tumors Predict Clinical Outcome. *Science*, *313*(5795), 1960–1964. https://doi.org/10.1126/science.1129139

Galon, J., Fridman, W. H., & Pages, F. (2007). The adaptive immunologic microenvironment in colorectal cancer: A novel perspective. In *Cancer Research* (Vol. 67, Issue 5, pp. 1883–1886). https://doi.org/10.1158/0008-5472.CAN-06-4806

Gao, W., Xiong, Y., Li, Q., & Yang, H. (2017). Inhibition of toll-like receptor signaling as a promising therapy for inflammatory diseases: A journey from molecular to nano therapeutics. In *Frontiers in Physiology* (Vol. 8, Issue JUL). Frontiers Media S.A. https://doi.org/10.3389/fphys.2017.00508

Giraldo, N. A., Becht, E., Remark, R., Damotte, D., Sautès-Fridman, C., & Fridman, W. H. (2014). The immune contexture of primary and metastatic human tumours. In *Current Opinion in Immunology* (Vol. 27, Issue 1, pp. 8–15). Elsevier Ltd. https://doi.org/10.1016/j.coi.2014.01.001

González-Silva, L., Quevedo, L., & Varela, I. (2020). Tumor Functional Heterogeneity Unraveled by scRNA-seq Technologies. In *Trends in Cancer* (Vol. 6, Issue 1, pp. 13–19). Cell Press. https://doi.org/10.1016/j.trecan.2019.11.010

Hekmati, M., Polak-Charcon, S., & Ben-Shaul, Y. (1990). A morphological study of a human adenocarcinoma cell line (HT29) differentiating in culture. Similarities to intestinal embryonic development. *Cell Differentiation and Development*, 207–218.

Hellmann, M. D., Ciuleanu, T.-E., Pluzanski, A., Lee, J. S., Otterson, G. A., Audigier-Valette, C., Minenza, E., Linardou, H., Burgers, S., Salman, P., Borghaei, H., Ramalingam, S. S., Brahmer, J., Reck, M., O'Byrne, K. J., Geese, W. J., Green, G., Chang, H., Szustakowski, J., … Paz-Ares, L. (2018). Nivolumab plus Ipilimumab in Lung Cancer with a High Tumor Mutational Burden. *New England Journal of Medicine*, *378*(22), 2093–2104. https://doi.org/10.1056/nejmoa1801946

Hodi, F. S., O'Day, S. J., McDermott, D. F., Weber, R. W., Sosman, J. A., Haanen, J. B., Gonzalez, R., Robert, C., Schadendorf, D., Hassel, J. C., Akerley, W., van den Eertwegh, A. J. M., Lutzky, J., Lorigan, P., Vaubel, J. M., Linette, G. P., Hogg, D., Ottensmeier, C. H., Lebbé, C., … Urba, W. J. (2010). Improved Survival with Ipilimumab in Patients with Metastatic Melanoma. *New England Journal of Medicine*, *363*(8), 711–723. https://doi.org/10.1056/nejmoa1003466

Huang, Q.-Q., & Pope, R. M. (2009). The Role of Toll-like Receptors in Rheumatoid Arthritis. *Current Rheumatology Reports*, *11*, 357–364.

Huang, Y., Tian, C., Li, Q., & Xu, Q. (2019). TET1 knockdown inhibits porphyromonas gingivalis LPS/IFN-γ-induced M1 macrophage polarization through the NF-κb pathway in THP-1 cells. *International Journal of Molecular Sciences*, *20*(8). https://doi.org/10.3390/ijms20082023

Jaffee, E. M., Hruban, R. H., Biedrzycki, B., Laheru, D., Schepers, K., Sauter, P. R., Goemann, M., Coleman, J., Grochow, L., Donehower, R. C., Lillemoe, K. D., O'Reilly, S., Abrams, R. A., Pardoll, D. M., Cameron, J. L., & Yeo, C. J. (2001). Novel Allogeneic Granulocyte-Macrophage Colony-Stimulating Factor-Secreting Tumor Vaccine for Pancreatic Cancer: A Phase I Trial of Safety and Immune Activation. *Journal of Clinical Oncology*, *19*(1), 145–156.

Jarnicki, A. G., Lysaght, J., Todryk, S., & Mills, K. H. G. (2006). Suppression of Antitumor Immunity by IL-10 and TGF-Producing T Cells Infiltrating the Growing Tumor: Influence of Tumor Environment on the Induction of CD4 and CD8 Regulatory T Cells 1. In *The Journal of Immunology* (Vol. 177).

Jezierska, A., Kolosova, I. A., & Verin, A. D. (2011). Toll Like Receptors Signaling Pathways as a Target for Therapeutic Interventions. In *Current Signal Transduction Therapy* (Vol. 6).

Jialal, I., Kaur, H., & Devaraj, S. (2014). Toll-like receptor status in obesity and metabolic syndrome: A translational perspective. *Journal of Clinical Endocrinology and Metabolism*, *99*(1), 39–48. https://doi.org/10.1210/jc.2013-3092

Kaczanowska, S., Joseph, A. M., & Davila, E. (2013). TLR agonists: our best frenemy in cancer immunotherapy . *Journal of Leukocyte Biology*, *93*(6), 847–863. https://doi.org/10.1189/jlb.1012501

Killock, D. (2015). Haematological cancer: Resiquimod-a topical CTCL therapy. In *Nature Reviews Clinical Oncology* (Vol. 12, Issue 10, p. 563). Nature Publishing Group. https://doi.org/10.1038/nrclinonc.2015.142

Kirkwood, J. M., Strawderman, M. H., Ernstoff, M. S., Smith, T. J., Borden, E. C., & Blum, R. H. (1996). Interferon Alfa-2b Adjuvant Therapy of High-Risk Resected Cutaneous Melanoma: The Eastern Cooperative Oncology Group Trial EST 1684. In *J Clin Oncol* (Vol. 14).

Klemm, F., Maas, R. R., Bowman, R. L., Kornete, M., Soukup, K., Nassiri, S., Brouland, J. P., Iacobuzio-Donahue, C. A., Brennan, C., Tabar, V., Gutin, P. H., Daniel, R. T., Hegi, M. E., & Joyce, J. A. (2020). Interrogation of the Microenvironmental Landscape in Brain Tumors Reveals Disease-Specific Alterations of Immune Cells. *Cell*, *181*(7), 1643-1660.e17. https://doi.org/10.1016/j.cell.2020.05.007

Kraaij, M. D., Savage, N. D. L., Van Der Kooij, S. W., Koekkoek, K., Wang, J., Van Den Berg, J. M., Ottenhoff, T. H. M., Kuijpers, T. W., Holmdahl, R., Van Kooten, C., & Gelderman, K. A. (2010). Induction of regulatory T cells by macrophages is dependent on production of reactive oxygen species. *Proceedings of the National Academy of Sciences of the United States of America*, *107*(41), 17686–17691. https://doi.org/10.1073/pnas.1012016107

Krishnan, M. A., Yadav, K., & Chelvam, V. (2021). Agarose Micro-Well Platform for Rapid Generation of Homogenous 3D Tumor Spheroids. *Current Protocols*, *1*(7). https://doi.org/10.1002/cpz1.199

Leach, D. R., Krummel, M. F., & Allison, J. P. (1996). *Enhancement of Antitumor Immunity by CTLA-4 Blockade*. https://www.science.org

Lee, D. W., Kochenderfer, J. N., Stetler-Stevenson, M., Cui, Y. K., Delbrook, C., Feldman, S. A., Fry, T. J., Orentas, R., Sabatino, M., Shah, N. N., Steinberg, S. M., Stroncek, D., Tschernia, N., Yuan, C., Zhang, H., Zhang, L., Rosenberg, S. A., Wayne, A. S., & Mackall, C. L. (2015). T cells expressing CD19 chimeric antigen receptors for acute lymphoblastic leukaemia in children and young adults: A phase 1 dose-escalation trial. *The Lancet*, *385*(9967), 517–528. https://doi.org/10.1016/S0140-6736(14)61403-3

Levings, M. K., Bacchetta, R., Schulz, U., & Roncarolo, M. G. (2002). The role of IL-10 and TGF-beta in the differentiation and effector function of T regulatory cells. In *International archives of allergy and immunology* (Vol. 129, Issue 4, pp. 263–276). https://doi.org/10.1159/000067596

Li, H., Somiya, M., & Kuroda, S. (2021). Enhancing antibody-dependent cellular phagocytosis by Re-education of tumor-associated macrophages with resiquimod-encapsulated liposomes. *Biomaterials*, *268*. https://doi.org/10.1016/j.biomaterials.2020.120601

Li, T. T., Ogino, S., & Qian, Z. R. (2014). Toll-like receptor signaling in colorectal cancer: Carcinogenesis to cancer therapy. *World Journal of Gastroenterology*, *20*(47), 17699–17708. https://doi.org/10.3748/wjg.v20.i47.17699

Liou, G. Y., & Storz, P. (2010). Reactive oxygen species in cancer. In *Free Radical Research* (Vol. 44, Issue 5, pp. 479–496). https://doi.org/10.3109/10715761003667554

Liu, P., Chen, G., & Zhang, J. (2022). A Review of Liposomes as a Drug Delivery System: Current Status of Approved Products, Regulatory Environments, and

Future Perspectives. In *Molecules* (Vol. 27, Issue 4). MDPI. https://doi.org/10.3390/molecules27041372

Lu, L., Ling, W., & Ruan, Z. (2021). TAM-derived extracellular vesicles containing microRNA-29a-3p explain the deterioration of ovarian cancer. *Molecular Therapy - Nucleic Acids*, *25*, 468–482. https://doi.org/10.1016/j.omtn.2021.05.011

Maeda, H., & Khatami, M. (2018). Analyses of repeated failures in cancer therapy for solid tumors: poor tumor-selective drug delivery, low therapeutic efficacy and unsustainable costs. *Clinical and Translational Medicine*, *7*(1). https://doi.org/10.1186/s40169-018-0185-6

McNally, A. K., & Anderson, J. M. (2011). *Macrophage Fusion and Multinucleated Giant Cells of Inflammation* (pp. 97–111). https://doi.org/10.1007/978-94-007-0763-4_7

Meyer, T., Surber, C., French, L. E., & Stockfleth, E. (2013). Resiquimod, a topical drug for viral skin lesions and skin cancer. *Expert Opinion on Investigational Drugs*, *22*(1), 149–159. https://doi.org/10.1517/13543784.2013.749236

Miller, S. A., Ghobashi, A., & O'hagan, H. M. (2021). Consensus molecular subtyping of colorectal cancers is influenced by goblet cell content. *Cancer Genetics*, 34–39. https://doi.org/10.1101/2020.11.17.387035

Mills, C. D. (2012). M1 and M2 Macrophages: Oracles of Health and Disease. In *Critical Reviews ™ in Immunology* (Vol. 32, Issue 06).

Mirlekar, B. (2022). Tumor promoting roles of IL-10, TGF-β, IL-4, and IL-35: Its implications in cancer immunotherapy. In *SAGE Open Medicine* (Vol. 10). SAGE Publications Ltd. https://doi.org/10.1177/20503121211069012

Montero Vega, M. T., & de Andrés Martín, A. (2009). The significance of toll-like receptors in human diseases. *Allergologia et Immunopathologia*, *37*(5), 252–263. https://doi.org/10.1016/j.aller.2009.04.004

Morgan, R. A., Dudley, M. E., Wunderlich, J. R., Hughes, M. S., Yang, J. C., Sherry, R. M., Royal, R. E., Topalian, S. L., Kammula, U. S., Restifo, N. P., Zheng, Z., Nahvi, A., De

Vries, C. R., Rogers-Freezer, L. J., Mavroukakis, S. A., & Rosenberg, S. A. (2016). *Cancer Regression in Patients After Transfer of Genetically Engineered Lymphocytes*. https://www.science.org

Multhoff, G., Molls, M., & Radons, J. (2012). Chronic inflammation in cancer development. In *Frontiers in Immunology* (Vol. 2, Issue JAN). https://doi.org/10.3389/fimmu.2011.00098

Ning, X., Yu, Y., Shao, S., Deng, R., Yu, J., Wang, X., She, X., Huang, D., Shen, X., Duan, W., Duan, J., & Zhang, H. (2021). The prospect of immunotherapy combined with chemotherapy in patients with advanced non-small cell lung cancer: a narrative review. *Annals of Translational Medicine*, *9*(22), 1703–1703. https://doi.org/10.21037/atm-21-4878

Padrón, L. J., Maurer, D. M., O'Hara, M. H., O'Reilly, E. M., Wolff, R. A., Wainberg, Z. A., Ko, A. H., Fisher, G., Rahma, O., Lyman, J. P., Cabanski, C. R., Yu, J. X., Pfeiffer, S. M., Spasic, M., Xu, J., Gherardini, P. F., Karakunnel, J., Mick, R., Alanio, C., … Vonderheide, R. H. (2022). Sotigalimab and/or nivolumab with chemotherapy in first-line metastatic pancreatic cancer: clinical and immunologic analyses from the randomized phase 2 PRINCE trial. *Nature Medicine*, *28*(6), 1167–1177. https://doi.org/10.1038/s41591-022-01829-9

Pagès, F., Mlecnik, B., Marliot, F., Bindea, G., Ou, F. S., Bifulco, C., Lugli, A., Zlobec, I., Rau, T. T., Berger, M. D., Nagtegaal, I. D., Vink-Börger, E., Hartmann, A., Geppert, C., Kolwelter, J., Merkel, S., Grützmann, R., Van den Eynde, M., Jouret-Mourin, A., … Galon, J. (2018). International validation of the consensus Immunoscore for the classification of colon cancer: a prognostic and accuracy study. *The Lancet*, *391*(10135), 2128–2139. https://doi.org/10.1016/S0140-6736(18)30789-X

Pahlavanneshan, S., Sayadmanesh, A., Ebrahimiyan, H., & Basiri, M. (2021). Toll-Like Receptor-Based Strategies for Cancer Immunotherapy. In *Journal of Immunology Research* (Vol. 2021). Hindawi Limited. https://doi.org/10.1155/2021/9912188

Pan, D., & Jia, D. (2021). Application of Single-Cell Multi-Omics in Dissecting Cancer Cell Plasticity and Tumor Heterogeneity. In *Frontiers in Molecular Biosciences* (Vol. 8). Frontiers Media S.A. https://doi.org/10.3389/fmolb.2021.757024

Park, J. H., Lee, J. M., Lee, E. J., Kim, D. J., & Hwang, W. B. (2018). Kynurenine promotes the goblet cell differentiation of HT-29 colon carcinoma cells by modulating Wnt, Notch and AhR signals. *Oncology Reports*, *39*(4), 1930–1938. https://doi.org/10.3892/or.2018.6266

Pauli, G., Chao, P.-H., Qin, Z., Böttger, R., Lee, S. E., Li, S.-D., Qin, Z. ;, Böttger, R. ;, Lee, S. E. ;, Li, S.-D., Kim, D.-H., & Marianecci, C. (2021). Liposomal Resiquimod for Enhanced Immunotherapy of Peritoneal Metastases of Colorectal Cancer. *Pharmaceutics*. https://doi.org/10.3390/pharmaceutics

Peng, H. Y., Lucavs, J., Ballard, D., Das, J. K., Kumar, A., Wang, L., Ren, Y., Xiong, X., & Song, J. (2021). Metabolic Reprogramming and Reactive Oxygen Species in T Cell Immunity. In *Frontiers in Immunology* (Vol. 12). Frontiers Media S.A. https://doi.org/10.3389/fimmu.2021.652687

Porter, D. L., Levine, B. L., Kalos, M., Bagg, A., & June, C. H. (2011). Chimeric Antigen Receptor–Modified T Cells in Chronic Lymphoid Leukemia. *New England Journal of Medicine*, *365*(8), 725–733. https://doi.org/10.1056/nejmoa1103849

Rapoport, A. P., Stadtmauer, E. A., Binder-Scholl, G. K., Goloubeva, O., Vogl, D. T., Lacey, S. F., Badros, A. Z., Garfall, A., Weiss, B., Finklestein, J., Kulikovskaya, I., Sinha, S. K., Kronsberg, S., Gupta, M., Bond, S., Melchiori, L., Brewer, J. E., Bennett, A. D., Gerry, A. B., … June, C. H. (2015). NY-ESO-1-specific TCR-engineered T cells mediate sustained antigen-specific antitumor effects in myeloma. *Nature Medicine*, *21*(8), 914–921. https://doi.org/10.1038/nm.3910

Robbins, P. F., Morgan, R. A., Feldman, S. A., Yang, J. C., Sherry, R. M., Dudley, M. E., Wunderlich, J. R., Nahvi, A. V., Helman, L. J., Mackall, C. L., Kammula, U. S., Hughes, M. S., Restifo, N. P., Raffeld, M., Lee, C. C. R., Levy, C. L., Li, Y. F., El-Gamil, M., Schwarz, S. L., … Rosenberg, S. A. (2011). Tumor regression in patients with

metastatic synovial cell sarcoma and melanoma using genetically engineered lymphocytes reactive with NY-ESO-1. *Journal of Clinical Oncology*, *29*(7), 917–924. https://doi.org/10.1200/JCO.2010.32.2537

Romano, E., Honeychurch, J., & Illidge, T. M. (2021). Radiotherapy-immunotherapy combination: How willwe bridge the gap between pre-clinical promise and effective clinical delivery? In *Cancers* (Vol. 13, Issue 3, pp. 1–23). MDPI AG. https://doi.org/10.3390/cancers13030457

Rook, A. H., Gelfand, J. C., Wysocka, M., Troxel, A. B., Benoit, B., Surber, C., Elenitsas, R., Buchanan, M. A., Leahy, D. S., Watanabe, R., Kirsch, I. R., Kim, E. J., & Clark, R. A. (2015). Topical resiquimod can induce disease regression and enhance T-cell effector functions in cutaneous T-cell lymphoma. *Blood*, *126*(12), 1452–1461. https://doi.org/10.1182/blood-2015-02-630335

Rosenberg, S. A., Lotze, M. T., Muul, L. M., Leitman, S., Chang, A. E., Ettinghausen, S. E., Matory, Y. L., Skibber, J. M., Shiloni, E., Vetto, J. T., Seipp, C. A., Simpson, C., & Reichert, C. M. (1985). Observations on the Systemic Administration of Autologous Lymphokine-Activated Killer Cells and Recombinant Interleukin-2 to Patients with Metastatic Cancer. *The New England Journal of Medicine*, *313*(23), 1485–1492.

Rosenberg, S. A., Packard, B. S., Aebersold, P. M., Solomon, D., Topalian, S. L., Toy, S. T., Simon, P., Lotze, M. T., Yang, J. C., Seipp, C. A., Simpson, C., Carter, C., Bock, S., Schwartzentruber, D., Wei, J. P., & White, D. E. (1988). Use of Tumor-Infiltrating Lymphocytes and Interleukin-2 in the Immunotherapy of Patients with Metastatic Melanoma. *The New England Journal of Medicine*, 1676–1680.

Rosenberg, S. A., & Restifo, N. P. (2015). *Adoptive cell transfer as personalized immunotherapy for human cancer*. https://www.science.org

Rosenberg, S. A., Spiess, P., & Lafreniere, R. (1986). A New Approach to the Adoptive Immunotherapy of Cancer with Tumor-Infiltrating Lymphocytes. *Science*, *233*, 1318–1321. https://www.science.org

Salgia, R., Lynch, T., Skarin, A., Lucca, J., Lynch, C., Jung, K., Hodi, F. S., Jaklitsch, M., Mentzer, S., Swanson, S., Lukanich, J., Bueno, R., Wain, J., Mathisen, D., Wright, C., Fidias, P., Donahue, D., Clift, S., Hardy, S., … Dranoff, G. (2003). Vaccination with irradiated autologous tumor cells engineered to secrete granulocyte-macrophage colony-stimulating factor augments antitumor immunity in some patients with metastatic non-small-cell lung carcinoma. *Journal of Clinical Oncology*, *21*(4), 624–630. https://doi.org/10.1200/JCO.2003.03.091

Schneider, G., Schmidt-Supprian, M., Rad, R., & Saur, D. (2017). Tissue-specific tumorigenesis: context matters. *Nature Reviews Cancer* , *12*, 239–253. https://doi.org/https://doi.org/10.1038/nrc.2017.5

Singh, N., Baby, D., Rajguru, J., Patil, P., Thakkannavar, S., & Pujari, V. (2019). Inflammation and cancer. *Annals of African Medicine*, *18*(3), 121–126. https://doi.org/10.4103/aam.aam_56_18

Sjoquist, K. M. (2023). Combination chemo-immunotherapy in advanced oesophageal squamous cell carcinoma. In *The Lancet Oncology* (Vol. 24, Issue 5, pp. 419–420). Elsevier Ltd. https://doi.org/10.1016/S1470-2045(23)00151-1

So, E. Y., & Ouchi, T. (2010). The application of Toll like receptors for cancer therapy. In *Int. J. Biol. Sci* (Vol. 6, Issue 7). http://www.biolsci.org675

Soiffer, R., Lynch, T., Mihm, M., Jung, K., Rhuda, C., Schmollinger, J. C., Hodi, F. S., Liebster, L., Lam, P., Mentzer, S., Singer, S., Tanabe, K. K., Cosimi, A. B., Duda, R., Sober, A., Bhan, A., Daley, J., Neuberg, D., Parry, G., … Dranoff, G. (1998). Vaccination with irradiated autologous melanoma cells engineered to secrete human granulocyte-macrophage colony-stimulating factor generates potent antitumor immunity in patients with metastatic melanoma. In *Immunology Communicated by Gertrude B. Elion* (Vol. 95). Glaxo Wellcome, Inc. www.pnas.org.

Spranger, S., & Gajewski, T. F. (2018). Impact of oncogenic pathways on evasion of antitumour immune responses. In *Nature Reviews Cancer* (Vol. 18, Issue 3, pp. 139–147). Nature Publishing Group. https://doi.org/10.1038/nrc.2017.117

Subramanian, S., Tus, K., Li, Q.-Z., Wang, A., Tian, X.-H., Zhou, J., Liang, C., Bartov, G., Mcdaniel, L. D., Zhou, X. J., Schultz, R. A., & Wakeland, E. K. (2006). *A Tlr7 translocation accelerates systemic autoimmunity in murine lupus*. www.ensembl.org.

Tsujimoto, H., Ono, S., Efron, P. A., Scumpia, P. O., Moldawer, L. L., & Mochizuki, H. (2008). Role of toll-like receptors in the development of sepsis. In *Shock* (Vol. 29, Issue 3, pp. 315–321). https://doi.org/10.1097/SHK.0b013e318157ee55

Tura, S., Baccarani, M., Zuffa, E., Russo, D., Fanin, R., Zaccaria, A., & Fiacchini, M. (1994). Interferon Alfa-2a as Compared with Conventional Chemotherapy for the Treatment of Chronic Myeloid Leukemia. *The New England Journal of Medicine*, 820–825.

Waldman, A. D., Fritz, J. M., & Lenardo, M. J. (2020). A guide to cancer immunotherapy: from T cell basic science to clinical practice. In *Nature Reviews Immunology* (Vol. 20, Issue 11, pp. 651–668). Nature Research. https://doi.org/10.1038/s41577-020-0306-5

WANG, C., XIE, J., GUO, J., MANNING, H. C., GORE, J. C., & GUO, N. (2012). Evaluation of CD44 and CD133 as cancer stem cell markers for colorectal cancer. *Oncology Reports*, *28*(4), 1301–1308. https://doi.org/10.3892/or.2012.1951

Wang, Q., Shao, X., Zhang, Y., Zhu, M., Wang, F. X. C., Mu, J., Li, J., Yao, H., & Chen, K. (2023). Role of tumor microenvironment in cancer progression and therapeutic strategy. In *Cancer Medicine* (Vol. 12, Issue 10, pp. 11149–11165). John Wiley and Sons Inc. https://doi.org/10.1002/cam4.5698

Wang, Y., Song, E., Bai, B., & Vanhoutte, P. M. (2016). Toll-like receptors mediating vascular malfunction: Lessons from receptor subtypes. In *Pharmacology and Therapeutics* (Vol. 158, pp. 91–100). Elsevier Inc. https://doi.org/10.1016/j.pharmthera.2015.12.005

Wei, C., Yang, C., Wang, S., Shi, D., Zhang, C., Lin, X., Liu, Q., Dou, R., & Xiong, B. (2019). Crosstalk between cancer cells and tumor associated macrophages is required

for mesenchymal circulating tumor cell-mediated colorectal cancer metastasis. *Molecular Cancer*, *18*(1). https://doi.org/10.1186/s12943-019-0976-4

Wellenstein, M. D., & de Visser, K. E. (2018). Cancer-Cell-Intrinsic Mechanisms Shaping the Tumor Immune Landscape. In *Immunity* (Vol. 48, Issue 3, pp. 399–416). Cell Press. https://doi.org/10.1016/j.immuni.2018.03.004

Wheeler, K. C., Jena, M. K., Pradhan, B. S., Nayak, N., Das, S., Hsu, C. D., Wheeler, D. S., Chen, K., & Nayak, N. R. (2018). VEGF may contribute to macrophage recruitment and M2 polarization in the decidua. *PLoS ONE*, *13*(1). https://doi.org/10.1371/journal.pone.0191040

Wong, S. W., Kwon, M. J., Choi, A. M. K., Kim, H. P., Nakahira, K., & Hwang, D. H. (2009). Fatty acids modulate toll-like receptor 4 activation through regulation of receptor dimerization and recruitment into lipid rafts in a reactive oxygen species-dependent manner. *Journal of Biological Chemistry*, *284*(40), 27384–27392. https://doi.org/10.1074/jbc.M109.044065

Wu, J. (2021). The enhanced permeability and retention (Epr) effect: The significance of the concept and methods to enhance its application. In *Journal of Personalized Medicine* (Vol. 11, Issue 8). MDPI. https://doi.org/10.3390/jpm11080771

Xu, F., Cui, W. Q., Wei, Y., Cui, J., Qiu, J., Hu, L. L., Gong, W. Y., Dong, J. C., & Liu, B. J. (2018). Astragaloside IV inhibits lung cancer progression and metastasis by modulating macrophage polarization through AMPK signaling. *Journal of Experimental and Clinical Cancer Research*, *37*(1). https://doi.org/10.1186/s13046-018-0878-0

Yang, Q., Guo, N., Zhou, Y., Chen, J., Wei, Q., & Han, M. (2020). The role of tumor-associated macrophages (TAMs) in tumor progression and relevant advance in targeted therapy. In *Acta Pharmaceutica Sinica B* (Vol. 10, Issue 11, pp. 2156–2170). Chinese Academy of Medical Sciences. https://doi.org/10.1016/j.apsb.2020.04.004

Yu, L., & Feng, Z. (2018). The Role of Toll-Like Receptor Signaling in the Progression of Heart Failure. In *Mediators of Inflammation* (Vol. 2018). Hindawi Limited. https://doi.org/10.1155/2018/9874109

Yunna, C., Mengru, H., Lei, W., & Weidong, C. (2020). Macrophage M1/M2 polarization. In *European Journal of Pharmacology* (Vol. 877). Elsevier B.V. https://doi.org/10.1016/j.ejphar.2020.173090

Zhang, Y., Choksi, S., Chen, K., Pobezinskaya, Y., Linnoila, I., & Liu, Z. G. (2013). ROS play a critical role in the differentiation of alternatively activated macrophages and the occurrence of tumor-associated macrophages. *Cell Research*, *23*(7), 898–914. https://doi.org/10.1038/cr.2013.75

Zhang, Y., & Liang, C. (2016). Innate recognition of microbial-derived signals in immunity and inflammation. In *Science China Life Sciences* (Vol. 59, Issue 12, pp. 1210–1217). Science in China Press. https://doi.org/10.1007/s11427-016-0325-6

Zhang, Y., & Zhang, Z. (2020). The history and advances in cancer immunotherapy: understanding the characteristics of tumor-infiltrating immune cells and their therapeutic implications. In *Cellular and Molecular Immunology* (Vol. 17, Issue 8, pp. 807–821). Springer Nature. https://doi.org/10.1038/s41423-020-0488-6

Zhao, H., Wu, L., Yan, G., Chen, Y., Zhou, M., Wu, Y., & Li, Y. (2021). Inflammation and tumor progression: signaling pathways and targeted intervention. In *Signal Transduction and Targeted Therapy* (Vol. 6, Issue 1). Springer Nature. https://doi.org/10.1038/s41392-021-00658-5

Zhu, S., Zhang, T., Zheng, L., Liu, H., Song, W., Liu, D., Li, Z., & Pan, C. xian. (2021). Combination strategies to maximize the benefits of cancer immunotherapy. In *Journal of Hematology and Oncology* (Vol. 14, Issue 1). BioMed Central Ltd. https://doi.org/10.1186/s13045-021-01164-5